

# Origin of enriched-type mid-ocean ridge basalt at ridges far from mantle plumes: The East Pacific Rise at 11°20'N

Yaoling Niu and Ken D. Collerson

Department of Earth Sciences, The University of Queensland, Brisbane, Queensland, Australia

Rodey Batiza

Department of Geology and Geophysics, School of Ocean and Earth Science and Technology  
University of Hawaii, Honolulu

J. Immo Wendt and Marcel Regelous

Department of Earth Sciences, The University of Queensland, Brisbane, Queensland, Australia

**Abstract.** The East Pacific Rise (EPR) at 11°20'N erupts an unusually high proportion of enriched mid-ocean ridge basalts (E-MORB) and thus is ideal for studying the origin of the enriched heterogeneities in the EPR mantle far from mantle plumes. These basalts exhibit large compositional variations (e.g.,  $[La/Sm]_N = 0.68-1.47$ ,  $^{87}Sr/^{86}Sr = 0.702508-0.702822$ , and  $^{143}Nd/^{144}Nd = 0.513053-0.513215$ ). The  $^{87}Sr/^{86}Sr$  and  $^{143}Nd/^{144}Nd$  correlate with each other, with ratios of incompatible elements (e.g., Ba/Zr, La/Sm, and Sm/Yb) and with the abundances and ratios of major elements (TiO<sub>2</sub>, Al<sub>2</sub>O<sub>3</sub>, FeO, CaO, Na<sub>2</sub>O, and CaO/Al<sub>2</sub>O<sub>3</sub>) after correction for fractionation effect. These correlations are interpreted to result from melting of a two-component mantle with the enriched component residing as physically distinct domains in the ambient depleted matrix. The observation of  $[Nb/Th]_{PM} > 1$  and  $[Ta/U]_{PM} > 1$ , plus fractionated Nb/U, Ce/Pb, and Nb/La ratios, in lavas from the northern EPR region suggests that the enriched domains and depleted matrix both are constituents of recycled oceanic lithosphere. The recycled crustal/eclogitic lithologies are the major source of the enriched domains, whereas the recycled mantle/peridotitic residues are the most depleted matrix. On Pb-Sr isotope plot, the 11°20'N data form a trend orthogonal to the main trend defined by the existing EPR data, indicating that the enriched component has high  $^{87}Sr/^{86}Sr$  and low  $^{206}Pb/^{204}Pb$  and  $^{143}Nd/^{144}Nd$ . This isotopic relationship, together with mantle tomographic studies, suggests that the source material of 11°20'N lavas may have come from the Hawaiian plume. This "distal plume-ridge interaction" between the EPR and Hawaii contrasts with the "proximal plume-ridge interactions" seen along the Mid-Atlantic Ridge. The so-called "garnet signature" in MORB is interpreted to result from partial melting of the eclogitic lithologies. The positive Na<sub>8</sub>-Si<sub>8</sub>/Fe<sub>8</sub> and negative Ca<sub>8</sub>/Al<sub>8</sub>-Si<sub>8</sub>/Fe<sub>8</sub> trends defined by EPR lavas result from mantle compositional (vs. temperature) variation.

## 1. Introduction

It is widely accepted that mid-ocean ridges are mostly passive features in the sense that mantle upwelling beneath ridges results from plate separation. Mid-ocean ridge basalts (MORB), which represent the end product of decompression melting of the upwelling mantle, thus record the geochemical signatures of the uppermost mantle. Compared with basalts from other tectonic settings, MORB as a whole show relatively small geochemical variations, low abundances of incompatible elements, low radiogenic Sr and Pb, and high radiogenic Nd. These observations have led to the notion that oceanic upper mantle is relatively uniformly depleted in incompatible elements. The oceanic upper mantle has thus been designated as depleted MORB mantle (DMM) [Zindler and Hart, 1986], whose origin is

generally thought to have resulted from continental crust extraction in early Earth's history [e.g., Gast, 1968; O'Nions *et al.*, 1977]. The DMM itself, however, is compositionally heterogeneous, as incompatible element enriched-type (E-type) MORB occur at all ridges and in all ocean basins [e.g., Melson *et al.*, 1976]. The origin, history, and physical form of the enriched heterogeneities have been the subject of much research and speculation in the context of models of mantle circulation and ocean island basalt (OIB) genesis.

Most workers agree that mantle convection and crustal recycling are the primary mechanisms that create the enriched heterogeneities as "blobs" or "streaks" deep within the mantle that rise as plumes to supply OIB [e.g., Sun and Hanson, 1975; White and Hofmann, 1982; Allègre *et al.*, 1984; Thompson *et al.*, 1984; Allègre and Turcotte, 1986; Fitton and James, 1986; Hofmann *et al.*, 1986; Zindler and Hart, 1986; Saunders *et al.*, 1988; Hart and Zindler, 1989; Sun and McDonough, 1989; Weaver, 1991] and that the widespread E-type MORB reflect the presence of a diluted version of these OIB type materials in the subridge mantle [e.g., Dupré and Allègre, 1983; Thompson *et al.*, 1984; Allègre and Turcotte, 1986; Zindler and Hart, 1986; White *et al.*, 1987;

Copyright 1999 by the American Geophysical Union.

Paper number 1998JB900037.  
0148-0227/99/1998JB900037\$09.00

Saunders *et al.*, 1988; Mahoney *et al.*, 1994]. Indeed, MORB along many ridge segments in the Atlantic [Sun *et al.*, 1975; Schilling *et al.*, 1983; Dosso *et al.*, 1993; Taylor *et al.*, 1997] and Indian [Le Roex *et al.*, 1983, 1985] oceans show incompatible element enrichments whose amplitude increases with decreasing ridge axial depth toward on- and near-ridge hotspots (e.g., Iceland, Azores, and Bouvet) as the result of plume-ridge interactions. However, the origin of the ubiquitous E-type MORB along well-sampled portions (15°-5°N and 13°-23°S) of the East Pacific Rise (EPR) [e.g., Langmuir *et al.*, 1986; Macdougall and Lugmair, 1986; Thompson *et al.*, 1989; Natland, 1989; Hékinian *et al.*, 1989; Prinzhofer *et al.*, 1989; Sinton *et al.*, 1991; Batiza and Niu, 1992; Reynolds *et al.*, 1992; Perfit *et al.*, 1994; Mahoney *et al.*, 1994; Bach *et al.*, 1994; Niu *et al.*, 1996] is not readily explained by this plume-ridge interaction model because the EPR E-type MORB occur randomly and because of the apparent absence of mantle plumes/hotspots in the broad EPR region. Small-scale and large-amplitude geochemical variations in near-EPR seamount lavas have placed constraints on the enriched

heterogeneities as physically distinct domains of widespread but "spotty" dispersal in the ambient depleted MORB mantle [e.g., Batiza and Vanko, 1984; Zindler *et al.*, 1984; Niu *et al.*, 1996; Niu and Batiza, 1997a, b], with recycled oceanic crust as the probable ultimate origin [Niu and Batiza, 1997a].

In this paper, we present major and trace element data and Nd-Pb-Sr isotope results on 24 axial and off-axis MORB samples from the EPR at 11°20'N. Our data support previous interpretations on the size, distribution, and genesis of the enriched source heterogeneities in the sub-EPR mantle, but also provide clues on the ultimate origin of the mantle source heterogeneities in the context of mantle circulation. For example, our new data, plus the data from the near-ridge seamounts in the region [Niu and Batiza, 1997a], suggest that the enriched heterogeneities and ambient depleted matrix both are constituents of recycled oceanic lithosphere with the crustal lithologies as the major source of the enriched component and the previously melt-depleted peridotitic residues as the origin of the more depleted matrix. Furthermore, the new Nd-Pb-Sr isotope data suggest that

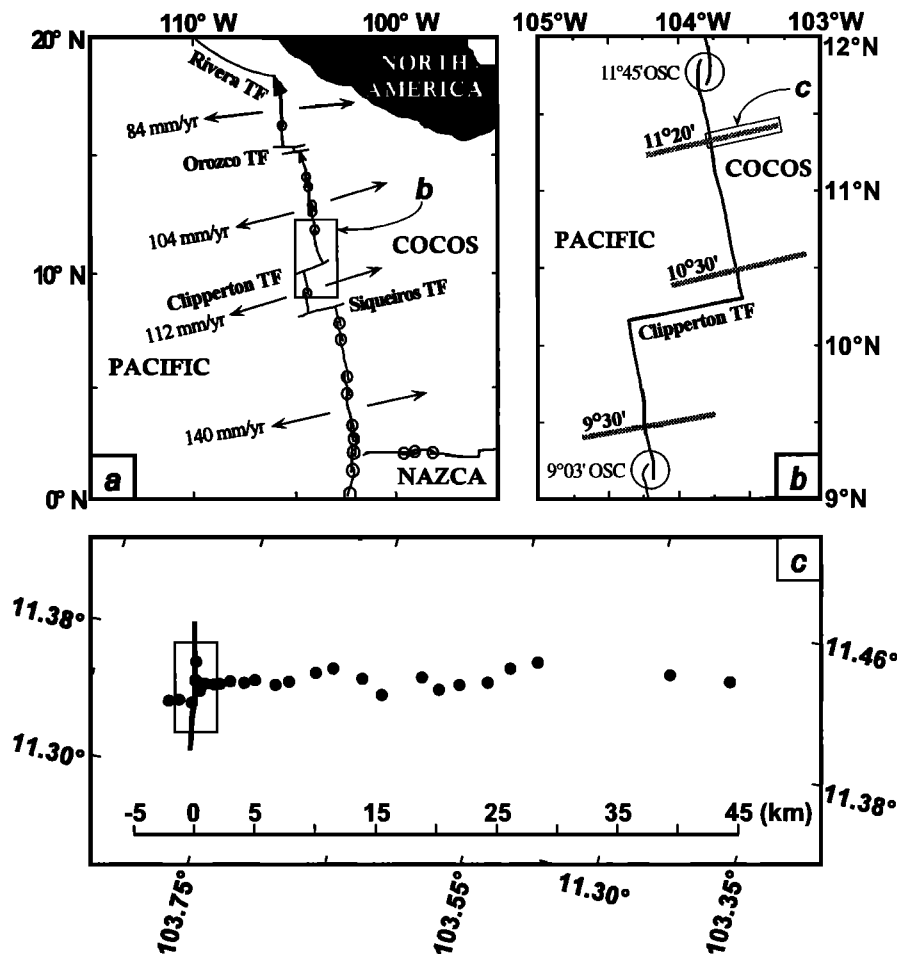


**Figure 1.** Schematic maps of (a) the northern East Pacific Rise (EPR), (b) sample locations, and (c) sample density. The bold lines at 9°30'N, 10°30'N, and 11°20'N are sampling traverses of the 1992 Phoenix 02 expedition [Batiza *et al.*, 1992, 1996]. We chose samples from the 11°20'N transverse on the Cocos plate in this study for two reasons: (1) The 11°20'N lavas show anomalous enrichment in incompatible elements (e.g., high K/Ti ratios) [Batiza *et al.*, 1992, 1996; Niu and Batiza, 1993b] suitable for studying the origin of enriched-type (E-type) mid-ocean ridge basalt (MORB); and (2) Samples from one side of the axis are sufficient for temporal coverage because major element data show symmetries on both sides of the axis along each traverse [Batiza *et al.*, 1996; Regelous *et al.*, 1997b], which suggests that lavas from the flanks were originally erupted close to the ridge axis, as confirmed by the  $^{40}\text{Ar}$ - $^{39}\text{Ar}$  dates on some of these samples [Duncan and Hogan, 1994].

traces of the Hawaiian plume may be discernible beneath the northern EPR. The great distance of transport from Hawaii to the EPR may explain both the spotty dispersal of the enriched heterogeneities and the absence of any thermal effects of the plume such as seafloor topography and ridge axial depth anomalies.

## 2. EPR at 11°20'N and Sample Locations

The samples are a subset of those collected during the 1992 Phoenix 02 expedition aboard R/V *Melville* [Batiza et al., 1992, 1996]. They are from the axis of the EPR at 11°20'N and off-axis along a flow line out to ~ 40 km (~ 800 ka) east of the axis on the Cocos plate (Figure 1 and Table 1). The axis at 11°20'N is magmatically the most robust area between the Clipperton and Orozco transforms and is characterized by a shallow axial depth (~2500 m), a broad axial region, a large summit cross-section area, and the existence of a magma lens reflector [e.g., Macdonald et al., 1988; Scheirer and Macdonald, 1993]. Unlike the rest of the well-sampled portions of the EPR (23°-13°S and 5°-15°N) [e.g., Langmuir et al., 1986; Sinton et al., 1991], the EPR at 11°20'N erupts an unusually high proportion of E-type MORB. For example, about half of the samples on and off axis at 11°20'N have  $K/Ti \geq 0.15$ , compared with less than 5% elsewhere along the EPR [Niu and Batiza, 1993b; Batiza et al., 1996]. The 11°20'N area is thus ideal for studying the nature and origin of mantle heterogeneity beneath the EPR.

## 3. Analytical Techniques

Major elements were determined on fresh glasses by electron microprobe at Lamont-Doherty Earth Observatory following the

procedure of Reynolds et al. [1992]. Trace elements were determined on hand-picked, phenocryst free, slightly leached (10% H<sub>2</sub>O<sub>2</sub>-5% HCl), and ultrasonically cleaned (mili-Q water), glass chips with a PQ2 Inductively-coupled mass spectrometer at The University of Queensland following Niu and Batiza [1997a]. Pb-Nd-Sr radiogenic isotopes were determined on similarly cleaned glass chips with a VG 54-30 Sector multicollector mass spectrometer at The University of Queensland following Regelous et al. [1997a]. Tables 2 and 3 present the data, with precisions on reference standards given in the table notes.

## 4. Data and Interpretations

### 4.1. Heterogeneous Parental Magmas: Evidence From Major and Minor Elements

Figure 2 shows that although fractional crystallization is important in causing some of the observed major and minor element compositional differences in the 11°20'N lavas, the large variations for most oxides at a given magnesium number (Mg<sup>#</sup>) indicate that these lavas were derived from compositionally different parental magmas. Compared with MORB from elsewhere on the EPR [e.g., Langmuir et al., 1986; Sinton et al., 1991; Batiza et al., 1996], the 11°20'N lavas as a whole have higher TiO<sub>2</sub>, Al<sub>2</sub>O<sub>3</sub>, Na<sub>2</sub>O, and K<sub>2</sub>O and slightly lower FeO and CaO at a given Mg<sup>#</sup>. These systematics and the variable and elevated K<sub>2</sub>O abundances and K/Ti ratios (0.13-0.37) argue for the presence of an anomalously enriched mantle beneath the EPR at 11°20'N. The small-scale and large-amplitude source compositional variation superimposed on the overall enriched mantle plays a key role in generating compositionally different parental magmas at 11°20'N.

### 4.2. A Two-Component Mantle: Evidence From Trace Elements and Sr and Nd Isotopes

Figure 3 shows that on incompatible element ratio-ratio plots the 11°20'N data form trends that lie on the arrays defined by near-EPR seamount data. These have been interpreted as melting-induced mixing arrays resulting from melting a two-component mantle [Niu and Batiza, 1997a, b]. Note that the seamount samples include the most enriched and the most depleted lavas so far discovered on the ocean floor thus providing constraints on the nature of the two end-member components in terms of incompatible trace elements [Niu and Batiza, 1997a]. Figure 4 shows that <sup>87</sup>Sr/<sup>86</sup>Sr and <sup>143</sup>Nd/<sup>144</sup>Nd of 11°20'N lavas exhibit a significant inverse correlation that lies within the "global" array, with the enriched end extending beyond the field defined by known EPR axial lavas (not shown). Both <sup>87</sup>Sr/<sup>86</sup>Sr and <sup>143</sup>Nd/<sup>144</sup>Nd correlate with ratios of incompatible elements as noted previously in this region [Zindler et al., 1984; Graham et al., 1988; Castillo et al., 1991; Niu et al., 1994]. Figures 3 and 4 suggest that the apparently complex mantle source heterogeneity beneath the northern EPR region is actually controlled mainly by two components. One component is relatively depleted and has high <sup>143</sup>Nd/<sup>144</sup>Nd and low <sup>87</sup>Sr/<sup>86</sup>Sr, Ba/Zr, Rb/Sr, Rb/Hf, Cs/Y, Nb/Sm, Nb/Hf, Ta/Ho, Ta/Hf, La/Sm, and Sm/Yb, while the other component is enriched, containing low <sup>143</sup>Nd/<sup>144</sup>Nd and high <sup>87</sup>Sr/<sup>86</sup>Sr, Ba/Zr, Rb/Sr, Rb/Hf, Cs/Y, Nb/Sm, Nb/Hf, Ta/Ho, Ta/Hf, La/Sm and Sm/Yb. These correlations also suggest that, regardless of the physical form of the enriched component in the immediate source region of these basalts, both components are ancient and have developed their isotopic characteristics independently for some time in excess of 1 Ga.

**Table 1.** Sample Locations of the 11°20'N EPR Lavas

Sample	Latitude, °N	Longitude, °W	Depth, m
PH82-1	11.43	103.38	2952
PH83-1	11.42	103.43	3014
PH84-1	11.41	103.53	3002
PH86-3	11.40	103.56	3000
PH88-1	11.38	103.59	2983
PH89-1	11.39	103.61	2960
PH90-2	11.37	103.64	2968
PH91-1	11.38	103.66	3063
PH92-1	11.38	103.68	2902
PH93-6	11.38	103.69	2934
PH94-1	11.37	103.71	2864
PH95-1	11.37	103.72	2883
PH97-2	11.36	103.74	2791
PH98-1	11.36	103.75	2815
PH99-2	11.36	103.76	2860
PH100-1	11.36	103.68	2626
PH101-1	11.35	103.77	2527
PHGC-60	11.35	103.77	2544
PH102-1	11.36	103.78	2587
PH103-1	11.37	103.78	2560
PH103-2	11.37	103.78	2560
PH104-1	11.34	103.78	2455
PHGC-22	11.34	103.79	2605
PH108-1	11.34	103.79	2681

Sample number prefix PH stands for 1992 Phoenix 02 expedition aboard R/V *Melville* [Batiza et al., 1992, 1996]. Latitude and longitude are fixed by the global positioning system (GPS). Depth, meters below sea level, is determined by Seabeam topography.

**Table 2.** Major and Trace Element Analyses of Glass Samples From 11°20'N EPR

Sample	82-1	83-1	84-1	86-3	88-1	89-1	90-2	91-1	92-1	93-6	94-1	95-1	97-2	
<i>Electron Microprobe Analyses at Lamont-Doherty Earth Observatory, wt%</i>														
SiO <sub>2</sub>	50.99	50.18	50.47	50.63	51.34	49.80	50.61	50.16	50.11	50.38	50.34	50.70	50.15	
TiO <sub>2</sub>	1.62	1.64	1.88	1.83	1.85	1.71	2.15	1.47	1.94	1.58	1.62	1.93	2.05	
Al <sub>2</sub> O <sub>3</sub>	15.24	15.60	15.20	15.39	14.57	16.10	14.97	15.79	16.04	15.08	15.26	15.12	14.53	
FeOt	9.33	9.51	10.16	9.90	10.14	9.26	10.54	9.51	9.39	9.81	9.89	10.18	11.25	
MnO	0.18	0.20	0.18	0.17	0.19	0.15	0.19	0.16	0.17	0.21	0.20	0.21	0.22	
MgO	7.27	7.49	7.09	7.21	7.11	7.59	6.17	7.58	7.03	7.51	7.42	6.74	6.74	
CaO	11.88	11.71	11.45	11.61	11.46	11.76	10.95	12.19	11.25	12.09	11.98	11.39	11.46	
Na <sub>2</sub> O	2.87	2.79	2.94	2.77	2.73	2.95	3.44	2.76	3.17	2.83	2.73	3.10	3.12	
K <sub>2</sub> O	0.20	0.23	0.24	0.26	0.17	0.27	0.54	0.13	0.48	0.21	0.21	0.29	0.19	
P <sub>2</sub> O <sub>5</sub>	0.20	0.18	0.20	0.18	0.19	0.19	0.33	0.13	0.28	0.16	0.15	0.25	0.21	
Sum	99.77	99.53	99.81	99.94	99.77	99.78	99.88	99.87	99.86	99.86	99.79	99.92	99.92	
Mg#	60.69	60.95	58.02	59.07	58.13	61.89	53.70	61.21	59.74	60.24	59.76	56.75	54.25	
<i>ICP-MS Analyses at The University of Queensland, ppm</i>														
Li	6.19	6.17	7.31	7.30	7.72	6.12	7.69	6.05	7.44	7.01	6.27	7.32	6.69	
Be	0.69	0.68	0.67	0.63	0.58	0.74	1.02	0.44	1.02	0.64	0.55	0.81	0.53	
Sc	44.6	41.6	44.4	42.5	47.9	40.9	44.5	42.3	43.6	43.7	43.5	43.6	41.4	
V	274	274	304	299	331	264	303	265	299	292	274	290	281	
Cr	333	323	234	313	245	297	148	336	264	253	306	155	143	
Co	49.0	51.2	51.5	50.6	47.8	48.3	45.2	50.1	50.0	46.8	46.6	45.9	41.4	
Ni	80.5	116	86.2	109	86.5	125	51.2	120	112	82.6	79.0	70.1	56.1	
Cu	87.0	87.8	80.6	78.5	80.7	80.9	81.6	82.3	82.3	79.3	84.0	77.4	75.3	
Zn	91.0	81.2	97.5	92.4	119	87.0	99.9	80.2	97.3	93.9	80.1	93.0	89.7	
Ga	17.9	18.4	19.4	19.2	19.3	19.3	21.5	18.2	22.1	18.9	18.1	19.2	17.2	
Rb	1.44	2.11	2.69	3.50	1.54	3.08	7.68	1.45	6.93	1.89	2.35	4.34	1.56	
Sr	176	187	185	177	131	212	211	142	287	156	143	170	129	
Y	27.8	27.9	31.4	31.1	38.3	27.9	35.5	27.2	33.1	33.2	28.2	33.7	32.7	
Zr	116	117	122	113	122	123	163	89.2	155	121	99	146	111	
Nb	5.17	6.58	5.90	7.02	3.29	7.01	14.3	2.99	13.82	4.92	5.99	9.49	3.92	
Cs	0.022	0.028	0.040	0.048	0.023	0.045	0.102	0.027	0.087	0.026	0.032	0.054	0.024	
Ba	16.0	23.1	29.7	46.1	15.0	34.8	85.0	12.2	87.2	19.6	24.2	41.5	15.8	
La	5.27	5.74	5.72	6.02	4.66	6.36	10.36	3.34	10.17	5.18	4.82	7.58	4.42	
Ce	15.6	15.8	16.8	16.6	14.2	18.0	26.2	10.4	26.3	15.7	13.4	20.5	13.4	
Pr	2.49	2.49	2.75	2.67	2.55	2.91	3.94	1.91	3.96	2.66	2.21	3.21	2.37	
Nd	11.6	11.6	13.0	12.6	12.7	13.3	17.6	9.62	17.3	12.7	10.7	14.5	11.8	
Sm	3.44	3.52	4.01	3.90	4.25	3.73	4.95	3.14	4.71	3.90	3.32	4.16	3.83	
Eu	1.28	1.27	1.46	1.38	1.45	1.36	1.70	1.18	1.69	1.41	1.21	1.44	1.37	
Gd	4.35	4.20	4.91	4.76	5.54	4.42	5.79	3.94	5.66	4.95	4.16	5.02	4.95	
Tb	0.74	0.71	0.83	0.83	0.99	0.76	0.95	0.72	0.94	0.88	0.74	0.90	0.86	
Dy	4.85	4.85	5.58	5.47	6.65	5.00	6.39	4.85	6.01	5.88	5.07	5.94	5.73	
Ho	1.05	1.04	1.18	1.18	1.43	1.04	1.32	1.03	1.24	1.24	1.07	1.24	1.21	
Er	2.95	2.85	3.27	3.20	3.91	2.75	3.53	2.72	3.39	3.48	2.88	3.37	3.44	
Tm	0.41	0.38	0.44	0.44	0.56	0.38	0.49	0.38	0.47	0.48	0.40	0.47	0.47	
Yb	2.73	2.64	3.02	3.01	3.76	2.65	3.36	2.63	3.23	3.34	2.81	3.33	3.22	
Lu	0.41	0.40	0.46	0.46	0.57	0.40	0.51	0.40	0.49	0.50	0.43	0.50	0.49	
Hf	2.64	2.59	2.91	2.75	3.00	2.68	3.56	2.14	3.46	2.83	2.35	3.07	2.75	
Ta	0.381	0.411	0.391	0.460	0.187	0.451	0.857	0.203	0.773	0.322	0.354	0.526	0.227	
Pb	0.564	0.544	0.618	0.596	0.521	0.635	0.987	0.359	0.958	0.558	0.449	0.730	0.487	
Th	0.251	0.317	0.314	0.391	0.220	0.383	0.815	0.141	0.760	0.260	0.313	0.556	0.213	
U	0.109	0.130	0.126	0.148	0.088	0.156	0.315	0.061	0.300	0.111	0.120	0.196	0.090	
Sample	98-1	99-2	100-1	101-1	GC-60	102-1	103-1	103-2	104-1	GC-22	108-1	VG-2	BIR-1	RSD
<i>Electron Microprobe Analyses at Lamont-Doherty Earth Observatory, wt%</i>														
SiO <sub>2</sub>	49.88	49.98	50.68	50.42	50.53	49.66	50.22	52.40	50.36	49.71	49.90	50.57		
TiO <sub>2</sub>	1.61	2.01	2.04	2.08	2.45	1.87	1.84	2.41	1.88	2.08	2.22	1.85		
Al <sub>2</sub> O <sub>3</sub>	15.78	14.87	14.35	14.50	14.33	15.28	15.27	13.78	15.06	15.80	15.93	14.06		
FeOt	9.84	11.51	11.07	11.22	11.94	10.74	10.40	12.48	10.51	10.18	10.16	11.59		
MnO	0.18	0.20	0.22	0.23	0.22	0.21	0.18	0.21	0.20	0.17	0.17	0.22		
MgO	7.56	6.70	6.50	6.69	6.02	7.24	7.15	4.78	7.12	6.92	6.46	7.07		
CaO	12.02	11.36	11.37	11.29	10.15	11.59	11.62	8.97	11.50	10.82	10.92	11.12		
Na <sub>2</sub> O	2.73	2.99	3.15	3.08	3.56	3.01	2.91	3.86	2.93	3.32	3.19	2.63		
K <sub>2</sub> O	0.15	0.20	0.23	0.22	0.46	0.19	0.19	0.57	0.23	0.55	0.60	0.19		
P <sub>2</sub> O <sub>5</sub>	0.15	0.19	0.19	0.18	0.27	0.18	0.17	0.35	0.19	0.28	0.27	0.20		
Sum	99.89	100.02	99.81	99.92	99.92	99.97	99.94	99.81	99.99	99.82	99.81	99.50		
Mg#	60.33	53.56	53.78	54.15	49.98	57.18	57.65	43.15	57.29	57.37	55.73	54.71		
<i>ICP-MS Analyses at The University of Queensland, ppm</i>														
Li	5.94	7.46	7.65	7.53	7.86	6.92	6.88	9.87	7.22	7.00	6.79		3.11	2.7
Be	0.47	0.63	0.67	0.68	0.95	0.60	0.58	1.39	0.65	0.89	0.90		0.091	8.8

Table 2. (continued)

Sample	98-1	99-2	100-1	101-1	GC-60	102-1	103-1	103-2	104-1	GC-22	108-1	VG-2	BIR-1	RSD
Sc	40.3	44.9	44.9	44.5	41.2	44.3	44.2	38.6	43.0	38.1	36.5		43.5	1.6
V	254	311	314	315	328	301	298	294	296	277	267		283	3.5
Cr	305	158	144	111	59.5	283	277	39.5	199	204	197		373	3.1
Co	48.0	46.9	47.7	46.4	42.0	47.7	47.3	40.7	48.0	45.4	44.1		55	7.1
Ni	118	69.0	76.3	58.3	45.3	91.3	91.3	34.7	84.5	104	102		170	2.1
Cu	76.4	76.2	77.3	76.2	86.6	74.3	74.7	79.1	74.6	72.7	69.5		121	2.2
Zn	83.1	92.4	97.6	96.7	114.9	90.9	89.3	116.7	93.6	88.2	88.0		66	3.9
Ga	17.7	19.4	19.5	19.3	20.1	18.9	18.9	24.0	19.3	20.5	19.8		15.4	2.3
Rb	1.38	2.11	2.22	2.24	6.23	2.08	2.02	8.08	2.68	7.61	7.45		0.2	4.4
Sr	151	155	156	155	198	156	153	183	156	273	270		109	1.3
Y	26.0	35.8	37.3	37.3	41.7	33.3	33.3	66.0	33.8	30.5	30.2		13.5	2.4
Zr	89	129	133	134	171	118	116	305	119	143	140		13.1	2
Nb	3.60	5.23	5.51	5.46	11.41	4.89	4.79	15.82	6.18	15.4	15.0		0.54	1.2
Cs	0.023	0.033	0.035	0.034	0.075	0.030	0.030	0.094	0.037	0.090	0.091		0.005	9.9
Ba	15.8	20.7	22.0	22.1	77.3	21.9	21.5	80.5	30.7	111	110		6.44	2.1
La	3.77	5.39	5.63	5.65	10.07	4.97	4.88	14.6	5.55	10.3	10.3		0.58	3.4
Ce	11.2	16.1	17.4	17.2	26.9	15.0	15.1	40.3	16.2	26.0	25.9		1.84	1.7
Pr	1.95	2.74	2.94	2.96	4.22	2.54	2.59	6.41	2.70	3.87	3.89		0.38	1.8
Nd	9.7	13.4	14.1	14.1	18.9	12.5	12.6	29.6	13.0	16.8	16.7		2.24	1.7
Sm	3.05	4.19	4.30	4.39	5.43	3.98	3.94	9.06	4.04	4.54	4.51		1.02	1.5
Eu	1.15	1.49	1.56	1.55	1.87	1.44	1.44	2.69	1.44	1.60	1.58		0.49	1.7
Gd	3.88	5.34	5.75	5.75	6.98	5.09	5.23	10.9	5.26	5.56	5.48		1.67	3.2
Tb	0.69	0.93	1.00	1.00	1.16	0.87	0.90	1.80	0.91	0.88	0.89		0.32	2.6
Dy	4.61	6.20	6.50	6.50	7.27	5.78	5.80	11.5	5.94	5.43	5.40		2.38	2.2
Ho	0.97	1.33	1.39	1.38	1.57	1.25	1.23	2.50	1.27	1.15	1.15		0.52	2.4
Er	2.71	3.69	3.96	3.89	4.92	3.49	3.55	7.08	3.54	3.20	3.19		1.54	2.5
Tm	0.37	0.50	0.56	0.56	0.64	0.49	0.50	1.02	0.51	0.45	0.45		0.22	2.1
Yb	2.64	3.50	3.77	3.81	4.08	3.19	3.27	6.48	3.31	2.92	2.93		1.49	2.8
Lu	0.38	0.53	0.55	0.56	0.89	0.48	0.48	1.00	0.50	0.44	0.45		0.22	2.1
Hf	2.18	3.06	3.27	3.23	4.08	2.90	2.86	7.37	2.86	3.25	3.22		0.53	1.8
Ta	0.226	0.313	0.376	0.333	0.680	0.286	0.299	0.904	0.360	0.823	0.815		0.049	1.1
Pb	0.455	0.504	0.582	0.570	0.967	0.499	0.693	1.090	0.551	0.907	0.903		2.81	3.1
Th	0.187	0.263	0.283	0.277	0.703	0.249	0.250	1.003	0.318	0.800	0.800		0.030	6.6
U	0.078	0.114	0.124	0.121	0.268	0.102	0.107	0.401	0.126	0.300	0.300		0.011	4.4

Major element analyses were done using electron microprobe at Lamont-Doherty Earth Observatory following Reynolds *et al.* [1992]; all these data were normalized to a Smithsonian MORB glass reference standard VG-2, whose working values were agreed upon by J. Karsten, E. Klein, and Y. Niu in 1993. FeOt is total Fe expressed as Fe<sup>2+</sup>. Mg<sup>#</sup> = Mg/[Mg+Fe<sup>2+</sup>] x 100 with 10% total Fe as Fe<sup>3+</sup>. Trace element analyses were done using a PQ2 Inductively-coupled mass spectrometer at The University of Queensland following Niu and Batiza [1997a]. The samples are fresh glass chips of 0.5-1.0 mm size hand-picked under a binocular microscope. U.S. Geological Survey reference standard BIR-1 is used at The University of Queensland as an unknown in each run with the reported values being the averages of 18 repeated analyses of 10 different sample digestions. RSD is the relative standard deviation in percentage. Readers are referred to Niu and Batiza [1997a] for sample preparation procedures, blank levels, detection limits, and analytical details.

### 4.3. Nature of the Enriched Component

**4.3.1. Evidence from trace element systematics.** The melting-induced mixing seen in Figures 3 and 4 involves either variable extents of melting of a two-component mantle or melting to similar extents of a mantle consisting of variable proportions of these two components or a scenario in between. The implications are (1) the enriched component exists as physically distinct domains in the ambient depleted mantle prior to major melting events, and (2) the size of these domains must be variably small and their distribution is not uniform. Furthermore, the fact, as demonstrated in Figure 5, that more enriched samples (i.e., higher [La/Sm]<sub>N</sub> (subscript "N" means chondrite normalized) have higher relative abundances of more incompatible elements (Ba > Nb > La > Zr > Y) suggests that these enriched domains may have trace element systematics consistent with their being of melt origin. That is, the enriched domains occur in the ambient depleted peridotitic matrix either as (1) dikes/veins resulting from prior low-degree melt metasomatic processes [e.g., Sun and Hanson, 1975; Hanson, 1977; Wood, 1979; Le Roex *et al.*, 1983, 1985; Zindler *et al.*, 1984; Sleep, 1984; Prinzhofer *et al.*, 1989; Sun and McDonough, 1989; Hirschmann and Stolper, 1996] or as

(2) fragments of recycled oceanic crust of basaltic composition (eclogitic in mineralogy) [e.g., Carmichael *et al.*, 1974; Allègre *et al.*, 1984; Hofmann and White, 1982; Saunders *et al.*, 1988; Hirschmann and Stolper, 1996; Niu and Batiza, 1997a].

**4.3.2. Evidence from correlated variations among major and trace elements and Sr isotopes.** Figure 6 shows that 11°20'N data exhibit statistically significant correlations among <sup>87</sup>Sr/<sup>86</sup>Sr, ratios of incompatible elements like [La/Sm]<sub>N</sub> and [Sm/Yb]<sub>N</sub>, and abundances and ratios of major elements after correction for fractionation to Mg<sup>#</sup> = 0.72 (Figure 7 and Table 4). Note that the data from the near-ridge seamounts in this region [Niu and Batiza, 1997a] show similar trends on [La/Sm]<sub>N</sub> and [Sm/Yb]<sub>N</sub> plots, suggesting that these correlations are of general significance and apply to the broad northern EPR region. The correlations between radiogenic isotopes and major elements such as Fe<sub>8</sub> and Na<sub>8</sub> (FeO and Na<sub>2</sub>O corrected to MgO = 8.0 wt%) have been observed previously in some northern EPR axial lavas [Castillo *et al.*, 1991; Batiza and Niu, 1992; Langmuir *et al.*, 1992; Niu *et al.*, 1996]. Niu *et al.* [1994, 1996] showed that, in fact, Ti<sub>8</sub>, Al<sub>8</sub>, Fe<sub>8</sub>, Ca<sub>8</sub>, Na<sub>8</sub>, and Ca<sub>8</sub>/Al<sub>8</sub> all correlate with radiogenic isotopes in some EPR lavas and interpreted these correlations as resulting from melting of a two-component mantle.

**Table 3.** Sr, Nd, and Pb Isotopic Compositions of Glass Samples From the EPR at 11°20'N

Sample	$^{87}\text{Sr}/^{86}\text{Sr}$	$^{143}\text{Nd}/^{144}\text{Nd}$	$\epsilon_{\text{Nd}}$	$^{206}\text{Pb}/^{204}\text{Pb}$	$^{207}\text{Pb}/^{204}\text{Pb}$	$^{208}\text{Pb}/^{204}\text{Pb}$
82-1	0.702511	0.513176	10.49	18.272 (18.288)	15.470 (15.477)	37.718 (37.740)
83-1	0.702528	0.513156	10.10	18.268	15.435	37.669
84-1	0.702599	0.513127	9.54	18.344 (18.316)	15.530 (15.492)	37.851 (37.749)
86-3	0.702657	0.513097	8.95	18.296	15.486	37.724
88-1	0.702544	0.513147	9.93	18.311	15.465	37.715
89-1	0.702538	0.513129	9.57	18.353	15.497	37.798
90-2	0.702757	0.513103	9.06	18.163 (18.167)	15.507 (15.507)	37.651 (37.642)
91-1	0.702607	0.513159	10.16	18.286 (18.294)	15.464 (15.473)	37.636 (37.663)
92-1	0.702795	-	-	18.199 (18.200)	15.500 (15.504)	37.647 (37.658)
93-6	0.702519	0.513190	10.76	18.328 (18.333)	15.488 (15.491)	37.773 (37.786)
94-1	0.702551	0.513105	9.11	18.433 (18.442)	15.493 (15.499)	37.890 (37.499)
95-1	0.702531	0.513156	10.10	18.441	15.509	37.965
97-2	0.702508	0.513175	10.48	18.187 (18.274)	15.457 (15.484)	37.575 (37.697)
98-1	0.702565	0.513166	10.29	18.304	15.475	37.722
99-2	0.702561	0.513142	9.84	18.327	15.474	37.676
100-1	0.702572	0.513133	9.65	18.344	15.491	37.764
101-1	0.702528	0.513215	11.25	18.356	15.509	37.817
GC-60	0.702659	0.513104	9.08	18.301 (18.276)	15.527 (15.497)	37.801 (37.688)
102-1	0.702555	0.513145	9.89	18.286	15.450	37.643
103-1	0.702571	0.513122	9.45	18.284	15.441	37.625
103-2	0.702656	0.513138	9.75	18.310	15.506	37.767
104-1	0.702659	0.513162	10.22	18.299	15.496	37.763
GC-22	0.702724	0.513059	8.21	18.212 (18.213)	15.506 (15.504)	37.658 (37.650)
108-1	0.702822	0.513053	8.10	18.192 (18.217)	15.489 (15.510)	37.616 (37.674)

All isotope measurements were done on a VG 54-30 Sector multicollector mass spectrometer at The University of Queensland. Nd was analyzed as metal ions in dynamic mode and corrected within run for mass fractionation using  $^{146}\text{Nd}/^{144}\text{Nd} = 0.7219$ . Sr was analyzed in dynamic mode and an exponential fractionation correction was applied using  $^{86}\text{Sr}/^{88}\text{Sr} = 0.1194$ . Mean values for the La Jolla Nd and NBS 987 Sr standards over the period of analyses were  $0.5118551 \pm 12$  and  $0.7102441 \pm 12$ , respectively. Total procedural blanks were less than 500 pg for Sr and Nd and were less than 200 pg for Pb. For Pb isotope analyses, mass fractionation was monitored by analysis of the NBS 981 Pb standard and was typically  $\sim 1.4\%$  per atomic mass unit. The errors on  $^{206}\text{Pb}/^{204}\text{Pb}$ ,  $^{207}\text{Pb}/^{204}\text{Pb}$ , and  $^{208}\text{Pb}/^{204}\text{Pb}$  are approximately  $\pm 0.007$ ,  $\pm 0.009$ , and  $\pm 0.03$ , respectively. Values in parentheses are repeated analyses for Pb isotopes. Readers are referred to *Regelous et al.* [1997a] for sample preparation, chemistry and analytical details.

The correlations in Figure 6 support this interpretation and provide additional insights into the nature of the enriched source materials and melting processes. As the relationship  $D_{\text{La}} < D_{\text{Sm}} < D_{\text{Yb}}$  is generally true during mantle melting regardless of detailed source mineralogy, high La/Sm and Sm/Yb ratios are thus expected in low-degree melts produced from an enriched source. Compared to the ambient depleted peridotitic matrix, incompatible element-enriched materials (either metasomatic veins/dikes or recycled oceanic crust) have high Rb/Sr (low Sm/Nd) ratios, high abundances of incompatible elements, and high volatile contents [Aggrey et al., 1988; Michael, 1995], they thus have lower melting temperatures and melt first [e.g., Kushiro et al., 1968; Mysen and Boettcher, 1975; Sleep, 1984; Zindler et al., 1984; Prinzhofer et al., 1989]. Hence the enriched materials dominate the composition (particularly, minor and trace incompatible elements) of the melt produced in the early stages (low degrees) of melting of a two-component mantle, and their proportions in the melt decrease with further (extensive) melting as a result of dilution [Niu et al., 1996]. Consequently, melts of low-degree melting are associated with high proportions of

enriched materials with inherited high  $^{87}\text{Sr}/^{86}\text{Sr}$  (low  $^{143}\text{Nd}/^{144}\text{Nd}$ ) ratios and high ratios of more incompatible over less incompatible elements (e.g., high K/Ti, La/Sm, and Sm/Yb) relative to melts of extensive melting. This interpretation is further substantiated by the major element data. For example, we know from peridotite melting experiments [Jaques and Green, 1980; Falloon et al., 1988; Baker and Stolper, 1994; Baker et al., 1995; Kushiro, 1996] that  $\text{TiO}_2$ ,  $\text{Al}_2\text{O}_3$ ,  $\text{Na}_2\text{O}$ ,  $\text{K}_2\text{O}$  and K/Ti in partial melts decrease, whereas FeO, CaO, and  $\text{CaO}/\text{Al}_2\text{O}_3$  increase with increasing degrees of melting.

#### 4.4. Intraoceanic Crust/Mantle Differentiation: The Origin of Both Enriched and Depleted End-members in the Northern EPR Mantle

**4.4.1 Evidence from fractionated Nb/U, Ce/Pb, Nb/La, and Nb/Ta ratios.** Hofmann et al. [1986] observed from the then available data that Nb/U and Ce/Pb ratios are uniform at  $47 \pm 10$  and  $25 \pm 5$ , respectively, in both MORB and OIB. They interpreted these uniform ratios as characterizing the mantle

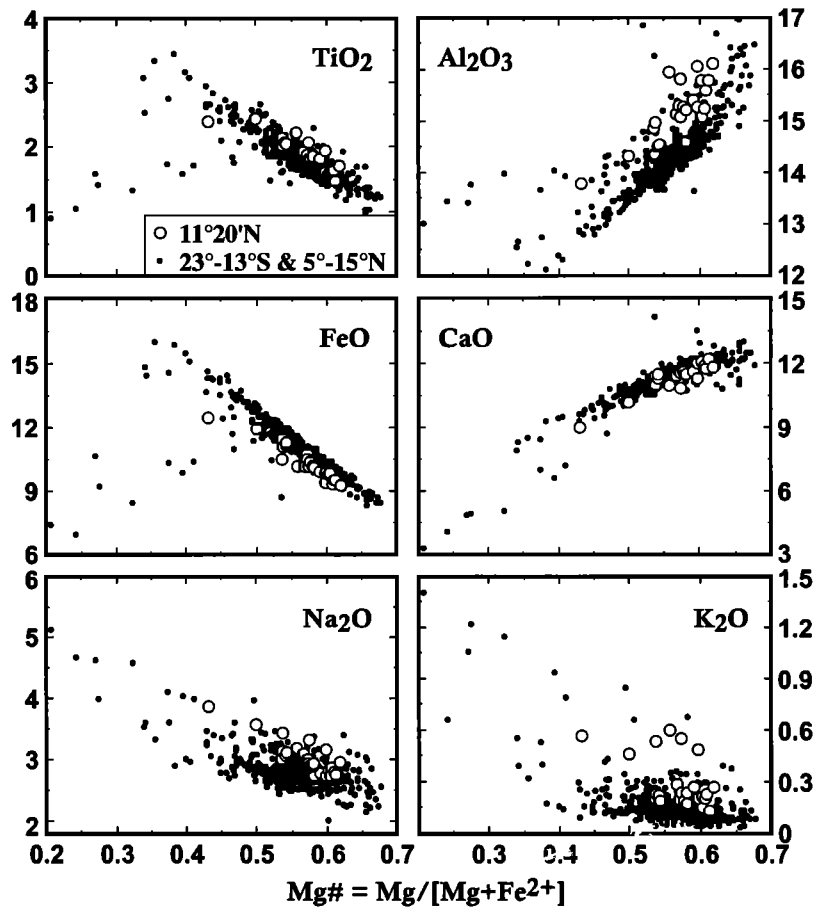


**Figure 2.** Magnesium number (Mg<sup>#</sup>) variation diagrams of representative major and minor elements of the 11°20'N EPR lavas. Group mean averages from well-sampled portions of the northern (5°-15°N) [Langmuir *et al.*, 1986; Batiza and Niu, 1992] and southern (13°- 23°S) [Sinton *et al.*, 1991] EPR are plotted for comparison.

sources of both types of oceanic basalts. These ratios are higher than Nb/U = ~ 30 and Ce/Pb = ~ 9 of the primitive mantle and are still higher than Nb/U = ~ 10 and Ce/Pb = ~ 4 of the average continental crust. In order to explain these observations, Hofmann *et al.* [1986] and Hofmann [1988, 1997] proposed that extraction of the major portion of the incompatible-element-enriched continental crust in Earth's early history, which fractionated Ce/Pb and Nb/U ratios, produced an incompatible-element-depleted, relatively homogeneous mantle from which the depleted source for MORB and the more enriched source of OIB were then produced without fractionating Ce/Pb and Nb/U ratios over a long period by the formation and subduction of oceanic crust. According to this model, low Ce/Pb and Nb/U ratios in oceanic basalts would be interpreted as source signatures involving continental crustal material (e.g., subduction of continent-derived sediments, etc.) in mantle sources of oceanic basalts.

While recycled continental crustal materials have been interpreted to exist in mantle sources of some oceanic basalts [e.g., Mahoney *et al.*, 1989; Klein and Karsten, 1995; White and Duncan, 1996; Hofmann, 1997], their overall contribution to the source of oceanic basalts is insignificant [Hofmann, 1988, 1997] because continental crust is too depleted in Nb and Ta relative to elements of similar incompatibility (e.g., Th and U) and has, for example, too low Nb/Sm, Nb/Hf, and Ta/Hf to be the enriched component for oceanic basalts as evident in Figure 3 [Niu and Batiza, 1997a, b]. Figure 8 shows that both Ce/Pb and Nb/U

ratios in some oceanic basalts, represented by the 11°20'N data and the data from the near-ridge seamounts in the region [Niu and Batiza, 1997a], are not uniform but vary significantly and systematically. On Ce/Pb versus Ce and Nb/U versus Nb plots, the data define positive trends with high Ce/Pb and Nb/U ratios for enriched samples and low Ce/Pb and Nb/U ratios for depleted samples. Note that the highly depleted samples have Ce/Pb ratios as low as, and Nb/U ratios lower than, the respective ratios of the primitive mantle. Clearly, the data trends on the two plots must result from processes that do not involve continental crustal material as the latter has Ce and Nb abundances that are too high, despite its very low Ce/Pb and Nb/U ratios, with respect to the data trends (Figures 8a and 8b). Therefore Ce/Pb and Nb/U ratios in oceanic basalts must be used with caution. Nb/La ratio in oceanic basalts has also been used similarly [e.g., Sun and McDonough, 1989; McDonough, 1991; Weaver, 1991] (perhaps because Nb and La could be reliably analyzed by conventional methods), but Figure 8c demonstrates that Nb is far more incompatible than La, and a large Nb/La variation is readily created during MORB genesis without providing reliable information on mantle source histories.

The important question now concerns the origin of the positive trends on Ce/Pb versus Ce, Nb/U versus Nb, and Nb/La versus Nb plots. We suggest that these trends are readily explained, as we interpreted above in Section 4.2, by melting-induced mixing of a two component mantle. The enriched component has high Ce and

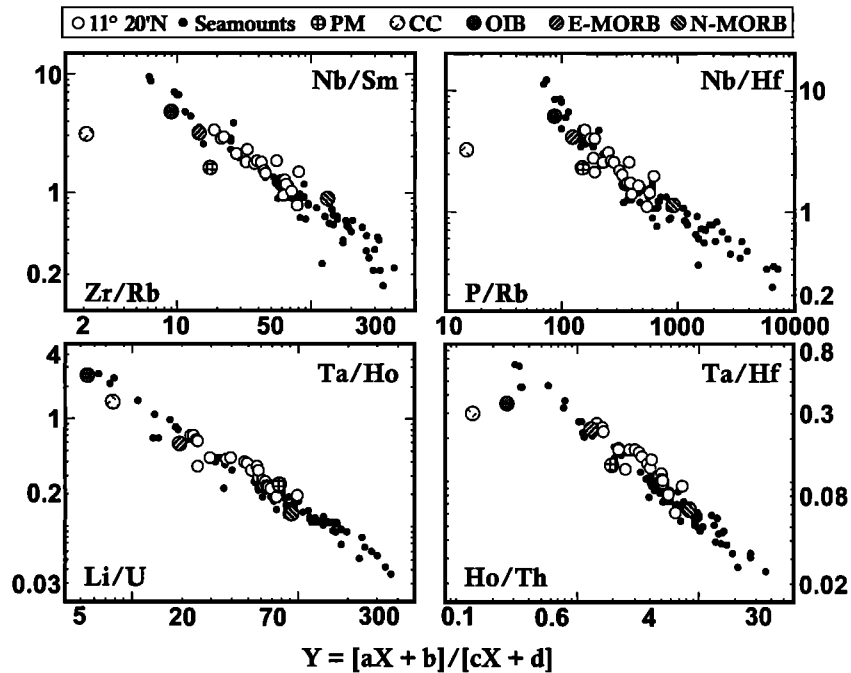


**Figure 3.** Representative incompatible element ratio-ratio plots showing that the 11°20'N data lie on the mixing trends defined by near-ridge seamount lavas [Niu and Batiza, 1997a]. Note that logarithmic scales are used for both axes to show the details and that the nonlinear trends described by the hyperbolic equation,  $Y = [aX + b]/[cX + d]$  (where  $Y$  and  $X$  are ratios of vertical and horizontal axes, and  $a - d$  are regression constants) result from the differences in relative incompatibility (i.e., the effect of melting) between the element in the numerator and the element in the denominator [Niu and Batiza, 1997a]. Therefore the mixing relationship is not simple binary mixing [e.g., Langmuir et al., 1978] but is melting-induced mixing, which is an inevitable geochemical consequence of melting a two-component mantle [e.g., Niu et al., 1996]. For comparison, average continental crust (CC) [Rudnick and Fountain, 1995], primitive mantle (PM), ocean island basalts (OIB), and both depleted N-MORB and enriched E-MORB [Sun and McDonough, 1989] are also shown.

Nb abundances, and Ce/Pb, Nb/U, and Nb/La ratios, whereas the depleted end-member has low Ce and Nb abundances and low Ce/Pb, Nb/U, and Nb/La ratios, consistent with all other incompatible element ratios [Niu and Batiza, 1997a]. The irrelevance of continental crustal materials to the data trends in Figures 3 and 8 suggests that the enriched component and depleted end-member both result from the same intraoceanic mantle differentiation in agreement with Hofmann et al. [1986]. We also agree that the major source of the enriched component is recycled oceanic crust. We suggest, however, that the extremely depleted end-member is recycled peridotitic residues formed beneath ancient ocean ridges by previous melt extraction events (including hot-spot melting residues). The positive trend on the Nb/Ta versus Nb plot (Figure 8d) supports this interpretation. Niu and Batiza [1997a] showed that Nb/Ta ratio in near-EPR seamount lavas is not constant, but decreases with decreasing Nb, and is as low as ~ 10 in the most depleted samples. Niu and Hékinian [1997, Figure 8] further demonstrated that Nb/Ta ratios in abyssal peridotites (MORB residues) decrease systematically with increasing extent of melt depletion and are as low as 2. This indicates that the highly depleted basalts with low Nb/Ta must be derived from a highly depleted peridotite source with low Nb/Ta. The most likely candidate is thus depleted residual peridotite resulting from previous melting events, that is, recycled residual oceanic lithospheric mantle.

**4.4.2. Evidence from unfractionated Nb/Th and Ta/U ratios.** Niu and Batiza [1997a] suggested using Nb/Th and Ta/U

ratios in oceanic basalts to decipher mantle source histories because these two ratios do not fractionate during mantle melting beneath ocean ridges, at least in the northern EPR mantle, as demonstrated by the essentially zero slopes on Th/Nb versus Th and U/Ta versus U plots (Figures 8e and 8f). Thus Th/Nb and U/Ta variations in basalts are a source signature inherited from previous events. Figure 9, following Niu and Batiza [1997a], shows that all these basalts possess high Nb (vs. Th) and Ta (vs. U) relative to the primitive mantle, suggesting that mantle sources of all these oceanic basalts have excess Nb\* and Ta\*. As subduction-zone-related magma genesis is the only known process that can significantly fractionate Nb/Th and Ta/U ratios, as exemplified by the Tonga arc lavas, it is clear that subduction-zone processes must also be responsible for the excess Ta\* and Nb\* in the sources of oceanic basalts. Descending oceanic lithosphere in the subduction zone experiences a series of dehydration reactions that preferentially transfer more water-soluble Th and U (vs. water-insoluble Nb and Ta) from the downgoing slab to the overlying mantle wedge [Saunders et al., 1988; Sun and McDonough, 1989; McDonough, 1991; Pearce and Peate, 1995]. Consequently, the residual slab is relatively depleted in Th and U, and return of this slab to the source regions of oceanic basalts would give rise to the observed Nb and Ta enrichments in oceanic basalts [Saunders et al., 1988; Niu and Batiza, 1997a]. McDonough [1991] gave an excellent account of the geochemical consequence of subduction zone dehydration, but because of the use of the Nb/La ratio (see section 4.4.1), he had to

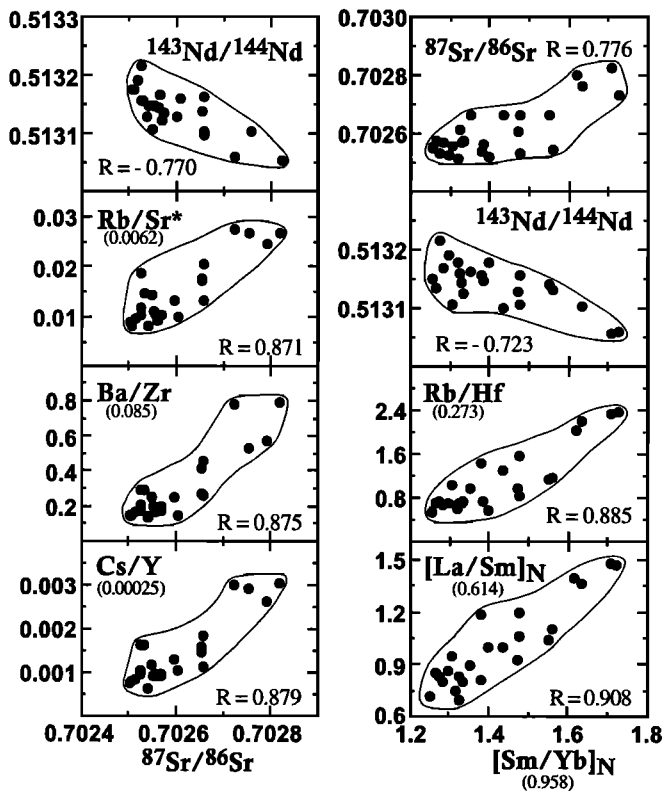


**Figure 4.** Representative plots showing significant correlations among radiogenic isotope ratios ( $^{87}\text{Sr}/^{86}\text{Sr}$  and  $^{143}\text{Nd}/^{144}\text{Nd}$ ), ratios of highly/moderately (e.g., Rb/Sr, Ba/Zr, Cs/Y, and Rb/Hf) and moderately/weakly (e.g.,  $[\text{Sm}/\text{Yb}]_N$ ) incompatible elements. These correlations are all statistically significant at  $> 99\%$  confidence level for  $N = 24$  samples. Note that  $[\text{Sm}/\text{Yb}]_N$  is commonly interpreted as a sensitive indicator for the presence of garnet as a residual phase in the melting mantle. The values in parentheses are ratios of the relevant elements in average N-MORB of *Sun and McDonough* [1989] to show that even the most depleted  $11^\circ 20'N$  samples are more enriched than average N-MORB. Note that we have 23 samples for  $^{143}\text{Nd}/^{144}\text{Nd}$ . The subscript "N" means chondrite normalized. Sr\* is Sr corrected for fractionation, that is,  $\text{Sr}^* = \text{Sr}_{\text{PM}} \times [\text{Pr}/\text{Pr}_{\text{PM}} + \text{Nd}/\text{Nd}_{\text{PM}}]/2$  by assuming  $D_{\text{Sr}} = [D_{\text{Pr}} + D_{\text{Nd}}]/2$  (where "PM" refers to primitive mantle values of corresponding elements [*Sun and McDonough*, 1989]).

conclude that a Nb-Ta-rich eclogitic reservoir did not exist in the sources of oceanic basalts but is hidden deep in the mantle. Note that Figure 9 also supports the idea that continental crust accretion is associated with arc magmatism [*Taylor and McLennan*, 1985].

The important point here is that oceanic basalts, including average OIB, E- and N-type MORB, highly enriched and extremely depleted seamount lavas, and Hawaiian lavas, all plot in the upper right quarter of Figure 9 with  $\text{Nb}^* > 1$  and  $\text{Ta}^* > 1$ . This suggests that the sources of probably most oceanic basalts, particularly those from the northern EPR region, were derived from materials previously recycled through subduction zones. The enriched and depleted source end-members must represent different parts of recycled oceanic lithosphere, with the crustal lithologies (eclogitic) as the ultimate origin of the enriched component and the depleted lithospheric mantle as the most likely candidate for the origin of the extremely depleted end-member.

As the extent of Th (vs. Nb) and U (vs. Ta) loss during subduction zone dehydration may not necessarily depend on lithologies (i.e., hydrothermally altered crust vs. serpentinized mantle peridotites), the Nb\* and Ta\* values in Figure 9 are thus not expected to correlate in any simple way with the absolute abundances of incompatible elements in the basalts. A Ti-rich phase (e.g., rutile) is commonly interpreted to exist in the subducted oceanic crust that retains Nb and Ta [e.g., *Saunders et al.*, 1988; *McDonough*, 1991]. It seems less likely that such a phase would exist in subducted residual peridotite. Given the low abundances of incompatible elements in bulk, clinopyroxene-absent, residual peridotites [*Niu and Hékinian*, 1997] and the water-insoluble nature of Nb and Ta (vs. Th, U and other incompatible elements) during dehydration, a particular Ti-rich phase in residual peridotites to host Nb and Ta (vs. Th and U) is apparently not needed.

It should be noted that recycled oceanic crust has been widely accepted to be important in causing mantle source heterogeneities, but the role of the melt-depleted peridotitic residues must also be considered. The oceanic lithospheric mantle is volumetrically ( $\geq 100$  km thick) far more significant than the crust ( $< 10$  km thick). The enriched crustal lithologies and the underlying depleted peridotitic residues both subduct and ultimately contribute to spatially small-scale and compositionally large-amplitude mantle heterogeneities. Over geological time, these two types of lithologies may be well stirred but not homogenized [e.g., *Morgan*

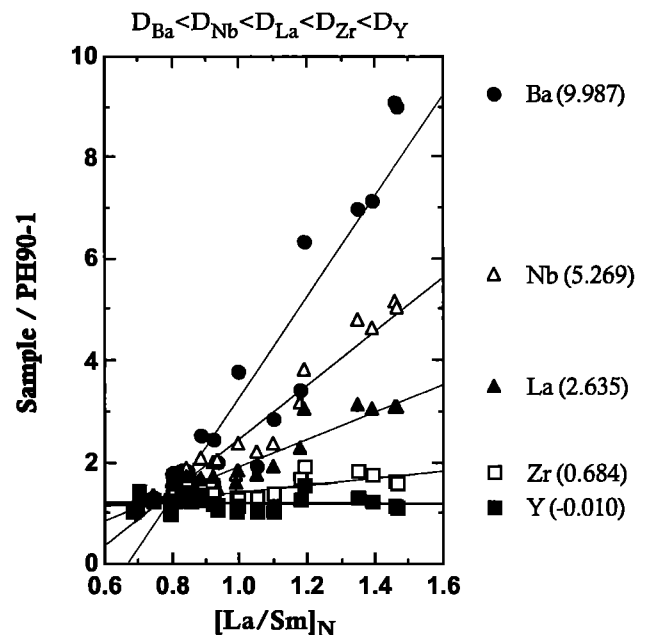


**Figure 5.** Plot of representative elements Ba, Nb, La, Zr, and Y normalized to the most depleted sample of the suite (PH90-1) as a function of  $[\text{La}/\text{Sm}]_N$ . As these elements have the relative incompatibility of  $D_{\text{Ba}} < D_{\text{Nb}} < D_{\text{La}} < D_{\text{Zr}} < D_{\text{Y}}$ , the increase in the regression slope (values in parenthesis) from Y to Ba suggests that more enriched samples with higher  $[\text{La}/\text{Sm}]_N$  have higher relative abundances of more incompatible elements (Ba  $>$  Nb  $>$  La  $>$  Zr  $>$  Y). This suggests that the enriched heterogeneities in the MORB melting region are of melt origin and occur either as dikes/veins resulting from prior low-degree melt metasomatic processes or as fragments of recycled oceanic crust (eclogite). Note that the most evolved sample PH103-2 is not plotted.

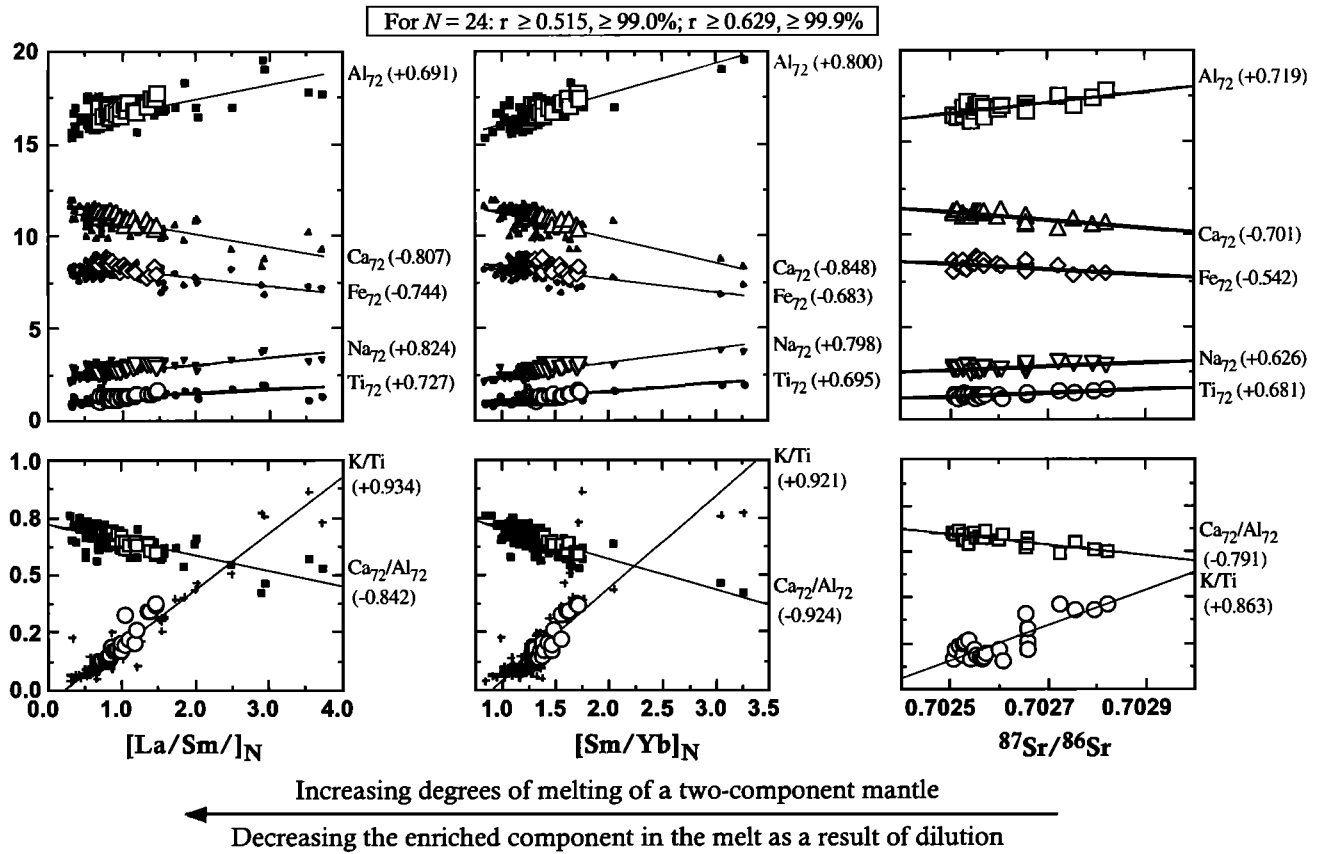


**Figure 6.** Plots of K/Ti and abundances and ratios of major elements after correction for fractionation to  $Mg^\# = 72$  against  $[La/Sm]_N$ ,  $[Sm/Yb]_N$ , and  $^{87}Sr/^{86}Sr$ . The scheme for fractionation correction is illustrated by Figure 7 and Table 4. Data from the seamounts in the region [Niu and Batiza, 1997a] are plotted using small symbols for comparison. The values in parentheses are correlation coefficients for  $11^\circ 20'N$  data only. Note that although the seamount data have much greater variations, the trends are the same as those defined by the  $11^\circ 20'N$  data. Note again that the “garnet signature”, as reflected by the varying  $[Sm/Yb]_N$ , correlates with major elements as well as ratios of incompatible trace elements and isotopes.

and Phipps Morgan, 1997; Phipps Morgan and Morgan, 1997], resulting in the development of the so-called “marble cake” structure [e.g., Allègre and Turcotte, 1986] of the two-component mantle [e.g., Zindler et al., 1984; Prinzhofer et al., 1989; Niu et al., 1996; Niu and Batiza, 1997a].

**4.5. Transport of Recycled Oceanic Lithospheric Material to the EPR Mantle: A Speculation Based on Pb Isotopes and Mantle Tomography**

The foregoing interpretation implies that both OIB and MORB would be compositionally similar if the enriched and depleted types of lithologies were uniformly distributed in the sources of oceanic basalts. This is clearly not the case. The fact that, in

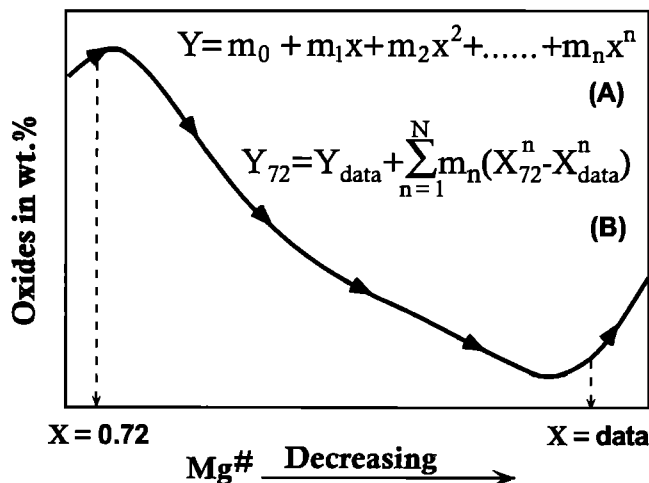


**Figure 7.** A schematic plot showing how the effect of crystal fractionation can be removed in order to examine elemental systematics in primary melts. The vertical axis is the element of interest, and the horizontal axis is  $Mg^\#$ . The curve, using  $Al_2O_3$  as an example, represents a liquid line of descent (LLD). The arrows along the curve point to decreasing temperature. A polynomial equation (A) for each oxide is determined using a large data set previously discussed elsewhere [Batiza and Niu, 1992; Niu et al., 1996; Niu and Batiza, 1997a], and the correction is to move all the data points backtracked along the LLD to  $Mg^\# = 72$  (denoted as a subscript 72) using equation (B). The  $n$  refers to the  $n$ th power of the polynomial term, and  $m_n$  is the coefficient of the  $n$ th term of the polynomial equation. The coefficients for oxides of interest are given in Table 4.

**Table 4.** Polynomial Coefficients for Correcting Fractionation Effect to Magnesium Number of 72

	SiO <sub>2</sub>	TiO <sub>2</sub>	Al <sub>2</sub> O <sub>3</sub>	FeO	CaO	Na <sub>2</sub> O
m <sub>0</sub>	5984.8	108.96	340.39	-199.04	-1850.3	183.71
m <sub>1</sub>	-69896	-1868.1	-3023.1	1650.9	22414	-1733.3
m <sub>2</sub>	338560	11955	10421	-4603.3	-111430	6550.1
m <sub>3</sub>	-863390	-37469	-15681	5497.7	292130	-12176
m <sub>4</sub>	1222900	62231	6860.7	-2407.1	-425880	11128
m <sub>5</sub>	-912410	-52752	6245	0.32139	327540	-4004.4
m <sub>6</sub>	280250	18005	-5375.4	-0.10119	-130900	0.18546

The polynomial coefficients m<sub>0</sub>, m<sub>1</sub>, m<sub>2</sub>, m<sub>3</sub>, m<sub>4</sub>, m<sub>5</sub>, m<sub>6</sub> were determined using Equation A in Figure 7, and were used to correct for fractionation effect to Mg<sup>#</sup> value of 72 using Equation B in Figure 7.

general, MORB are depleted in incompatible elements relative to OIB requires that the enriched lithologies are more abundant in the OIB source than in the MORB source. It is possible that in the course of the long history of mantle circulation, the enriched and depleted lithologies may have been somehow physically separated from each other and then became the sources of OIB and MORB, respectively. However, it seems physically more likely that hotspot melting of the two-component mantle produces incompatible element enriched OIB and that the residues of OIB melting (depleted in incompatible elements) become the source of MORB [e.g., *Morgan and Phipps Morgan, 1997; Phipps Morgan and Morgan, 1997*]. This suggests that while enriched and depleted lithologies of the two-component mantle are both ancient, the sources of some MORB may have acquired their depleted, dominantly peridotitic lithologies relatively recently as a

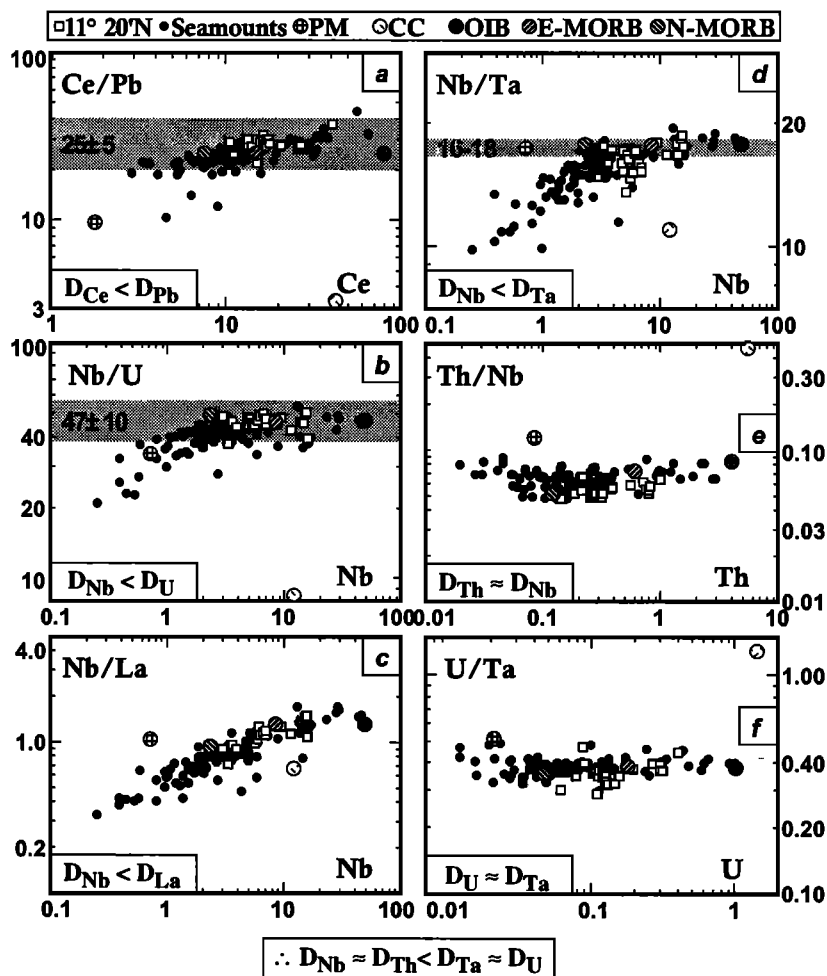


**Figure 8.** Ratio-element diagrams of 11°20'N data and the data from near-ridge seamounts in the region [Niu and Batiza, 1997a], with average continental crust (CC) [Rudnick and Fountain, 1995], primitive mantle (PM), OIB, and both N- and E-MORB [Sun and McDonough, 1989] plotted for reference. (a) Ce/Pb and (b) Nb/U ratios, which have been thought to be constant ( $25 \pm 5$  and  $47 \pm 10$ , respectively) in oceanic basalts [e.g., Hofmann et al., 1986], are not constant but decrease in progressively more depleted lavas. (c) The steep Nb/La versus Nb trend indicates that Nb is far more incompatible than La and a large Nb/La fractionation is readily produced during magma genesis without necessarily providing useful information on mantle source histories as commonly assumed. (d) Nb/Ta in oceanic basalts is not constant at 16 - 18 as previously believed but decreases progressively in more depleted lavas derived from highly depleted sources [Niu and Hékinian, 1997]. The essentially zero slopes on (e) Th/Nb versus Th and (f) Ta/U versus U plots demonstrate that these two ratios do not fractionate during magma genesis (i.e.,  $D_{Nb} \approx D_{Th} < D_{Ta} \approx D_U$ ); thus their values in oceanic basalts reflect their source ratios and provide important information on source histories.

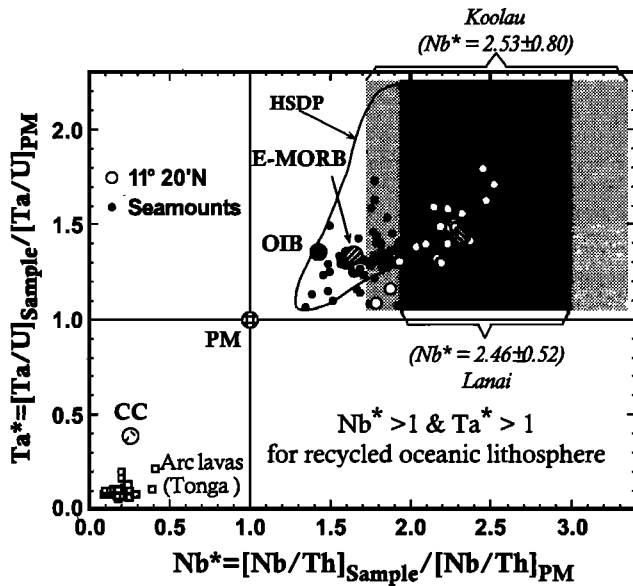


**Figure 9.**  $Ta^*$  versus  $Nb^*$  for  $11^{\circ}20'N$  samples. For comparison, samples from the nearby seamounts [Niu and Batiza, 1997a], average continental crust (CC) [Rudnick and Fountain, 1995], primitive mantle (PM), OIB, both E- and N-MORB [Sun and McDonough, 1989], and Tonga arc lava data [Ewart et al., 1998] are also plotted. The closed field HSDP represents Hawaii Scientific Drilling Project data (analyses with  $Nb/Ta > 12$  plotted) of Albarède [1996] and Hofmann and Jochum [1996]. The shaded regions represent the ranges of  $Nb^*$  for Hawaiian Koolau lavas (from Frey et al. [1994] with no U data available) and Lanai lavas (from West et al. [1992] with no Ta data available). Given the  $D_{Nb} \approx D_{Th} < D_{Ta} \approx D_U$  relationship [Niu and Batiza, 1997a] (also see Figure 8), the high  $Nb^*$  and  $Ta^*$  in these oceanic basalts are interpreted to indicate that the sources of these basalts are recycled oceanic lithosphere that had previously undergone subduction zone dehydration which preferentially transferred the Th and U (vs Nb and Ta) to the mantle wedge above for arc volcanism with the “residual” lithosphere enriched in Nb and Ta. Note that crustal and mantle peridotitic lithologies both undergo dehydration in the subduction zone, yet the extent of dehydration may not be lithology (crustal or peridotitic) dependent thus no simple relationship is expected on this diagram between  $Nb^*$  and  $Ta^*$  values and abundance levels of incompatible elements.

result of hotspot melting/depletion in the asthenosphere. A number of observations support this hypothesis. For example, MORB along the North Mid-Atlantic Ridge [e.g., Sun et al., 1975; Schilling et al., 1983; Dosso et al., 1993] show incompatible element enrichments whose amplitude increases systematically from N-type MORB at deep ridges to E-type MORB and even OIB compositions at shallow ridges toward on- and near-ridge hotspots (e.g., Iceland and Azores). The along-ridge depth variation and the geochemical signals, which are the thermal and chemical consequences of plume ridge interactions [e.g., Schilling, 1991; Ito and Lin, 1995; Ito et al., 1996; Ribe, 1996; Sleep, 1996], reflect the along-ridge asthenospheric flow of plume materials. The declining geochemical enrichment in erupted lavas in predicted direction of mantle flow results from the progressive depletion of the two-component plume source as a result of decompression melting during subridge passive mantle

upwelling. The “residual” plume source materials depleted in enriched lithologies may continue to flow, but the “familiar” enriched geochemical signals of plumes in erupted basalts diminish and are eventually replaced by “normal” depleted MORB. We interpret this model [after Morgan and Phipps Morgan, 1997] as “flow differentiation” of an initially two-component plume mantle in a ridge or near-ridge environment where lithosphere is young and thin and decompression melting is possible because of the ambient passive mantle upwelling beneath the ridge. This model is physically simple and is different from the commonly held view of plume-ridge interactions [e.g., Schilling, 1991; Pan and Batiza, 1998] which requires invasion of enriched plume materials in the preexisting depleted N-MORB mantle.

Compared to the Mid-Atlantic Ridge and ridges in the Indian Ocean, the ubiquitous E-type MORB along the EPR occur randomly in space and time [e.g., Langmuir et al., 1986; Sinton et al., 1991; Mahoney et al., 1994; Batiza et al., 1996; Janney and Castillo, 1997]. This observation and the apparent absence of mantle plumes in this broad EPR region suggest that mantle plume signals are rather attenuated in the EPR mantle. Nd-Pb-Sr isotope data for MORB from the Indian Ocean and South Atlantic suggest that plume signals can be discerned over thousands of kilometers from the plume source as a result of mantle flow over tens of millions of years in the convecting upper mantle [e.g., Hanan et al., 1986; Storey et al., 1989; Michael et al., 1994]. For example, the geochemical anomaly at  $33^{\circ}S$ , Mid-Atlantic Ridge, may represent a passive blob of the St. Helena or Bouvet plume [Michael et al., 1994]. Mahoney et al. [1994] speculated that the prominent isotopic “dome” at the southern EPR ( $15.8\text{--}20.7^{\circ}S$ ) may reflect source contamination by plume materials from the French Polynesian hotspots to the west. Likewise, the unusual Pb isotopes of the  $11^{\circ}20'N$  lavas suggest that the northern EPR mantle may, in fact, have been supplied by Hawaiian mantle plume material.

Figure 10 shows that whereas most of the data from the EPR plot in a field extending between the DMM and the HIMU (see Zindler and Hart [1986] for definition) mantle component with high radiogenic Pb-isotope ratios, the  $11^{\circ}20'N$  data form a distinct array orthogonal to the EPR trend. That is, the enriched component of the  $11^{\circ}20'N$  lavas has high radiogenic Sr and low radiogenic Pb and Nd, extending toward values for the bulk silicate earth (BSE) or the EM1 (see Zindler and Hart [1986] for definition) component or the broad field of Hawaiian plume materials, which themselves are isotopically very heterogeneous [e.g., Staudigel et al., 1984; West et al., 1992; Roden et al., 1994; Stille et al., 1986; Hauri, 1996]. Note that the overall range of the  $11^{\circ}20'N$  data is very limited and remains confined within the MORB field in the global context. However, it is the distinct, statistically significant trend that indicates that the enriched component must have low radiogenic Pb. Lavas of similar isotopic characteristics have been previously found at the EPR axis at  $6^{\circ}44'N$  [Hamelin et al., 1984] and at  $11^{\circ}30'N$  and  $13^{\circ}00'N$  [Prinzhofer et al., 1989].

It is possible that the enriched material simply represents an embedded, passive heterogeneity fortuitously brought to the region by mantle flow over time scales of  $\sim 1$  Ga. While this possibility cannot be ruled out, we suggest that the enriched material is derived ultimately from the Hawaiian hotspot. This possibility is supported by mantle tomographic studies [Zhang and Tanimoto, 1993], which show that globally ridgeward asthenospheric flow of low-viscosity plume materials may be a

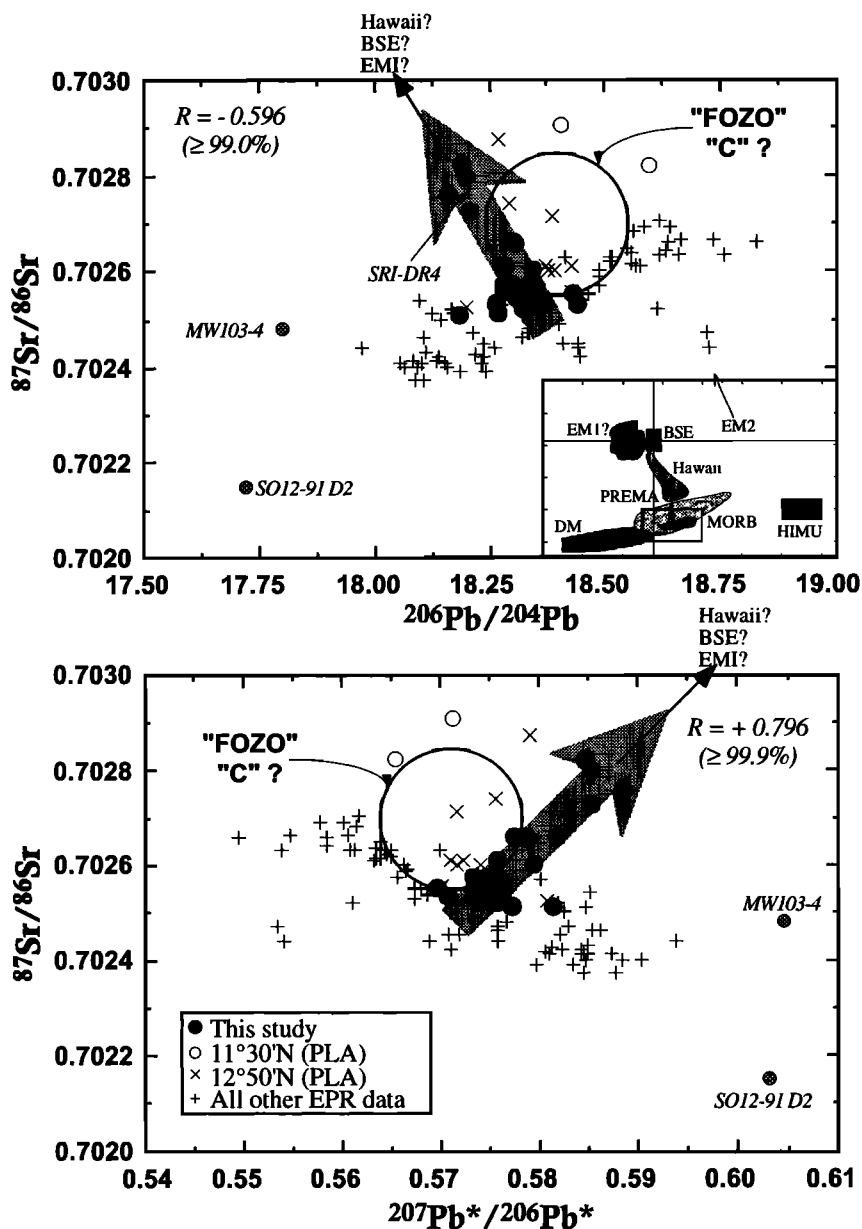


**Figure 10.** Plots of  $^{87}\text{Sr}/^{86}\text{Sr}$  against  $^{206}\text{Pb}/^{204}\text{Pb}$  and  $^{206}\text{Pb}^*/^{206}\text{Pb}^*$  to show that the  $11^\circ 20' \text{N}$  data (solid circles) form significant trends orthogonal to the array defined by the majority of the EPR axial data. That is, if the  $11^\circ 20' \text{N}$  array represents mixtures of the depleted MORB source and an enriched component as indicated by the trace element data, the enriched component would have high radiogenic Sr and low radiogenic Nd and Pb, remotely pointing to the field defined by the Hawaiian lavas [e.g., Staudigel *et al.*, 1984; Roden *et al.*, 1994; Stille *et al.*, 1986] or bulk silicate earth (BSE) or the enriched EM1 component of Zindler and Hart [1986]. The labeled circles may be the approximate positions of FOZO of Hart *et al.* [1992] or "C" of Hanan and Graham [1996]. The inset is a sketch simplified and modified from Zindler and Hart [1986] to show that the EPR data including the  $11^\circ 20' \text{N}$  data have very limited variation in the global context and that the Hawaiian plume itself is very heterogeneous as shown by the large field. The  $^{207}\text{Pb}^*/^{206}\text{Pb}^*$  is the ratio of the radiogenic components of  $^{207}\text{Pb}$  and  $^{206}\text{Pb}$  defined by Allègre *et al.* [1986]. The  $11^\circ 30' \text{N}$  and  $12^\circ 50' \text{N}$  data are from Prinzhofer *et al.* [1989]; SRI-DR4 (at  $6^\circ 44' \text{N}$ ) is from Hamelin *et al.* [1984]; all other EPR data are from Vidal and Clauer [1981], Cohen and O'Nions [1982], White and Hofmann [1982], Hamelin *et al.* [1984], White *et al.* [1987], Ito *et al.* [1987], Mahoney *et al.* [1994], and Bach *et al.* [1994]. SO12-91 D2 and MW103-4 are samples from the Garrett Transform analyzed by Hamelin *et al.* [1984] and Mahoney *et al.* [1994].

common phenomenon. Figure 11, simplified from Phipps Morgan *et al.* [1995], shows tomographic data from between Hawaii and the EPR and indicates the existence of a sublithospheric low-velocity zone connecting the Hawaiian plume and the EPR. Phipps Morgan *et al.* argue that plume flux from the deep mantle is the most important upward deep mantle flow balancing the downward flow of subduction and that this plume flux may feed mid-ocean ridges. This interpretation, while intriguing, is inconsistent with other models for the dispersal of plume material [Davies, 1988; Sleep, 1990; Schilling, 1991; Kincaid *et al.*, 1995; Ribe, 1996; Ito *et al.*, 1996] in the sense that other models require dispersed plume material to carry with it a thermal and density signal tracking its lateral flow from the hotspot.

The distance from Hawaii to the EPR is about 5000 km, over twice as far as any previously documented plume-influenced ridges [Schilling, 1991]. However, the great distance of transport, in fact, may explain both the spotty dispersal of the enriched heterogeneities and the absence of any thermal effects at the EPR. In previously documented cases, mantle plumes interact directly with ridges (e.g., Iceland) or with young, thin lithosphere near ridges (e.g., Azores, Galapagos, Easter, etc.), where plume materials (both enriched and depleted, we believe) flow laterally and undergo decompression melting in the ambience of passive mantle upwelling and hence result in erupted lavas showing an along-ridge geochemical gradient. This gradient can only be sustained for a distance limited by the amount of the enriched lithologies remaining in the flowing and melting plume mantle. In contrast, the Hawaiian plume interacts with old, thick lithosphere, and significant melting of the plume materials cannot therefore take place in the course of lateral asthenospheric

transport because of limited decompression. Consequently, both the enriched and depleted lithologies in the two-component Hawaiian plume mantle can survive transport to the EPR. What is seemingly counterintuitive in this proposal is the direction of the transport, which is opposite to the absolute plate motion of the Pacific plate. However, if this counter flow does not occur, then the alternative is upward vertical transport of high-viscosity material from below the low-velocity zone because materials must move up to fill the gap right beneath the ridge in response to plate separation. We suggest that passive lateral flow of low-viscosity materials through the low-velocity zone to feed a ridge is physically more likely than passive vertical flow of high-viscosity materials from greater depth. This hypothesis should be testable in terms of geophysical fluid dynamics.

Figure 12 plots  $[Sm/Yb]_N$  and  $^{87}Sr/^{86}Sr$  of the  $11^{\circ}20'N$  samples against eruption ages estimated from the spreading rate (see Figure 1c). Both patterns are similarly scattered, but the upper limits on both plots show a progressive increase from the background level some  $\sim 800$  ka ago to the peak level at present. This suggests that Hawaiian plume material may have arrived at the EPR rather recently, perhaps within the last 1 Ma. This, plus the fact that the EPR at  $11^{\circ}20'N$  has an unusually high portion of E-type MORB and is magmatically the most robust location between the Clipperton and Orozco transforms, may explain why the Hawaiian plume signature is not observed over a greater length of the EPR. As Hawaiian lavas, in general, have higher  $^3He/^4He$  than normal MORB [e.g., Kurz *et al.*, 1983; Roden *et al.*, 1994], helium isotope data as well as additional Pb isotope data on both axial and seamount samples from a larger area of the northern EPR region are required to test this hypothesis.

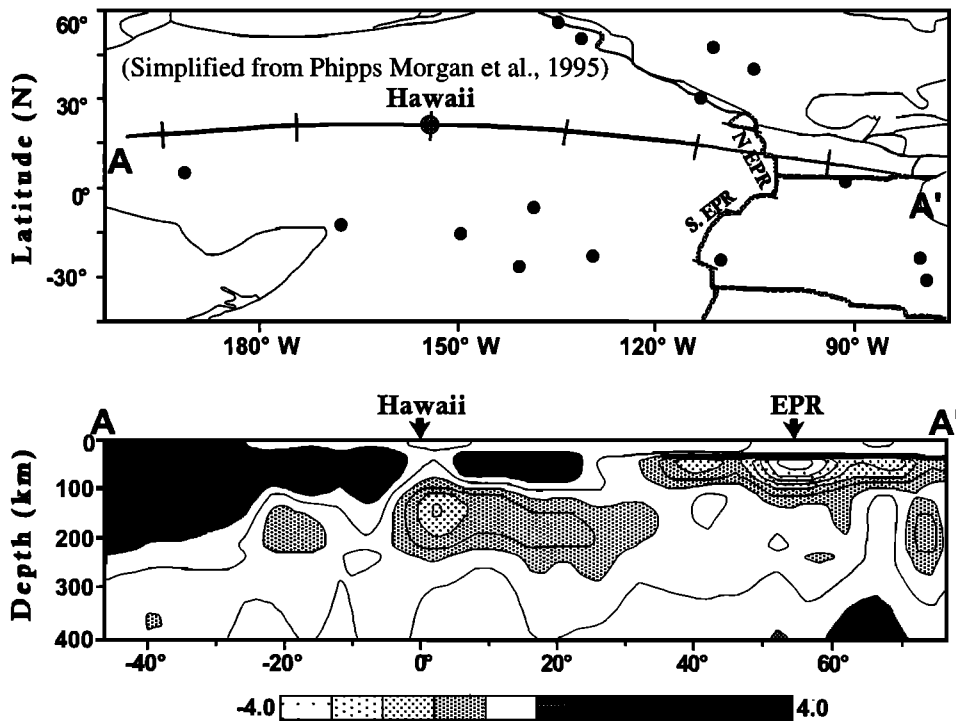


**Figure 11.** Simplified from Phipps Morgan *et al.* [1995]. (top) A portion of the global hotspot distribution (solid circles). (bottom) A vertical cross section of seismic shear velocity anomalies along a great circle path that connects the Hawaii hotspot and the EPR (profile A-A') [Zhang and Tanimoto, 1993]. Note that there exists a clear low-velocity layer at  $\sim 100$ -250 km depth beneath Hawaii that extends toward the East Pacific Rise to the east. Total velocity variation is  $\pm 4\%$ . Contour lines are at half the shading interval.

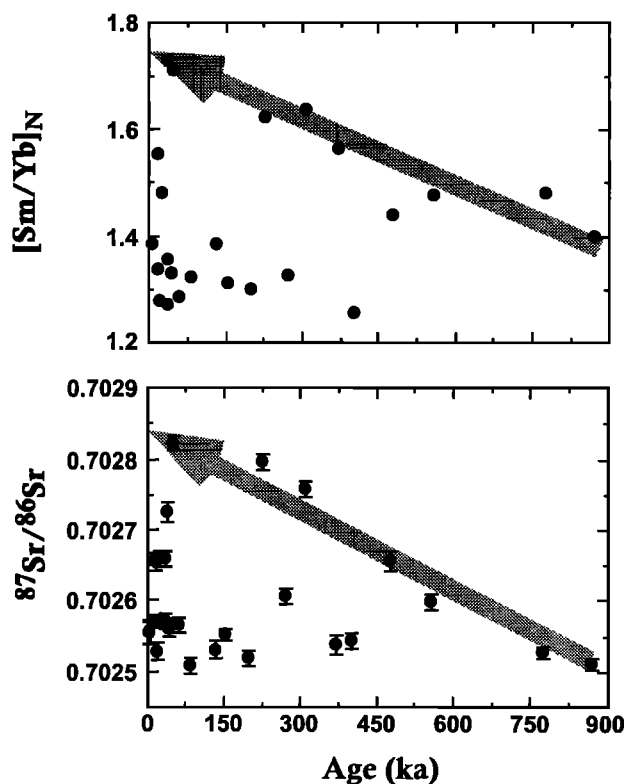


**Figure 12.** Plots of  $[Sm/Yb]_N$  and  $^{87}Sr/^{86}Sr$  of the  $11^{\circ}20'N$  lavas against lava eruption ages estimated from spreading rate ( $\sim 50$  mm/year half rate). Note that the upper limits on both plots increase since  $\sim 800$  ka, suggesting that the Hawaiian plume material may have arrived in the EPR mantle fairly recently.

#### 4.6. Summary of the Origin of E-Type MORB at $11^{\circ}20'N$ EPR in the Context of Mantle Circulation and Plume-Ridge Interactions

The data and foregoing discussion have shown that the abundant E-type MORB and the overall enriched nature of the lavas from the  $11^{\circ}20'N$  EPR (Figure 2) reflect the presence of an unusually enriched two-component mantle beneath this part of the EPR. The enriched component must occur as physically distinct domains in the ambient, highly depleted matrix. Melting to variable extents of such a two-component mantle or melting to similar extents of a mantle consisting of variable proportions of these two components leads to melting-induced mixing relationships in geochemical plots (see Figures 3, 4, 6, and 8). The observation that the more enriched lavas have higher relative abundances of more incompatible elements (Figure 5) indicates that the enriched domains are of melt origin either as dikes/veins resulting from prior low-degree melt metasomatic processes or as fragments of recycled oceanic crust. The fact that most of the oceanic basalts, represented by average OIB, E-type and N-type MORB, Hawaiian lavas, and both highly enriched and extremely depleted seamount lavas, show high  $Nb^*$  (vs. Th) and  $Ta^*$  (vs. U) (Figure 9) suggests that both the enriched domains and the depleted matrix are parts of recycled oceanic lithosphere that had experienced previous subduction zone dehydration during which the water-soluble Th and U had been preferentially transferred to the mantle wedge above for arc volcanism thus resulting in depletion of Th and U in the residual slab/lithosphere. Return of

the residual lithosphere to the sources of oceanic basalts, for example, beneath Hawaii and the northern EPR, thus gives rise to the excess  $Nb^*$  and  $Ta^*$  in these basalts.

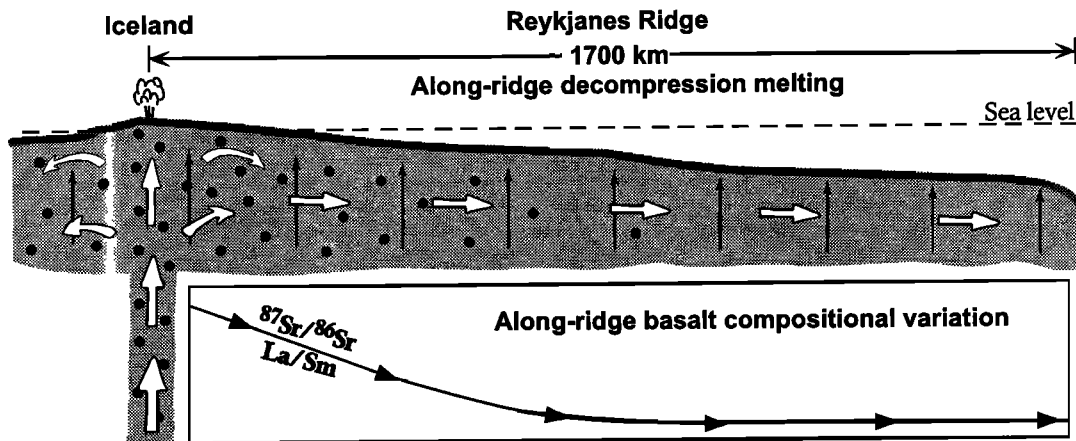
We interpret recycled oceanic crust (eclogitic) to be the major source of the enriched component and the recycled MORB (also OIB) melting residues (“abyssal peridotite”) underlying the crust to be the ultimate origin of the depleted end-member in the source of modern oceanic basalts at least beneath Hawaii and the northern EPR. During mantle circulation, these two types of lithologies may be well mixed, forming the “marble cake” structure of the two-component mantle. The exact pathways of how these recycled “composite” lithologies return to the sources of oceanic basalts would be debatable, depending on models of whether or not the subducting lithosphere can penetrate the 670 km seismic discontinuity and go down to the lower mantle (see *Christensen* [1995] for a review). Recent global mantle tomographic studies [e.g., *van der Hilst*, 1997] demonstrate that, indeed, subducting lithosphere can pass through the 670 km seismic discontinuity into the lower mantle and approach the core-mantle boundary. To balance this downward flow of subduction, upward mass transfer from the lower mantle to the upper mantle is required. It seems probable that plume flux from the deep mantle is the most important upward flow that feeds the upper mantle sources of oceanic basalts [*Phipps Morgan et al.*, 1995].

Hotspot melting of the two-component plume material produces incompatible element enriched OIB, creating residues that are variably depleted in the enriched component and which are the source of E- and N-type MORB [*Morgan and Phipps Morgan*, 1997. *Phipps Morgan and Morgan*, 1997]. This plume-ridge relationship is most obvious when plumes are spatially close to ridges, such as the Iceland plume - Reykjanes Ridge case in Figure 13, where buoyant upwelling and melting of the hot plume produces shallow ridge topography and enriched OIB-like basalts. The ambient subridge mantle upwelling allows the plume material flowing laterally beneath the ridge to melt, producing basalts whose amplitude of enrichment declines in the flow direction as the amount of the enriched component in the flowing plume source diminishes. The flow continues, but the “enriched” geochemical signals do not. As the Hawaiian plume is far away from the EPR, the plume-ridge interaction is rather passive. Lateral flow of the low-viscosity Hawaii plume material toward the EPR may be required by plate separation and lithosphere accretion at the EPR. This sublithospheric flow is deep and largely horizontal, so that decompression melting will not take place in the course of the flow, which allows the Hawaiian plume materials (both enriched and depleted) to be carried to the sub-EPR mantle (Figure 13).

#### 4.7. Additional Important Implications

**4.7.1. Role of metasomatic dikes/veins versus eclogites in the MORB source.** We suggested that the enriched component in the sources of northern EPR basalts occurs as physically distinct domains. These could be either fragments of recycled oceanic crust of eclogitic mineralogy or dikes/veins resulting from prior low-degree melt metasomatism, which may be ultimately derived from recycled eclogitic lithologies as well. The eclogites have compositions of subduction-zone-modified average oceanic crust, but the metasomatic dikes/veins would be extremely enriched in volatiles and incompatible elements. The two possible types of the enriched lithologies in the sources of oceanic basalts may not be distinguished from the erupted basalts because the geochemical

**"Proximal" plume-ridge interaction: Iceland Plume and Reykjanes Ridge**



Passive upwelling beneath the ridge causes decompression melting, which progressively depletes the enriched component in the flowing two-component plume mantle. This plume mantle depletion by "flow differentiation" explains the observed along-ridge basalt compositional variation.

**"Distal" plume-ridge interaction: Hawaii Plume and Northern EPR**

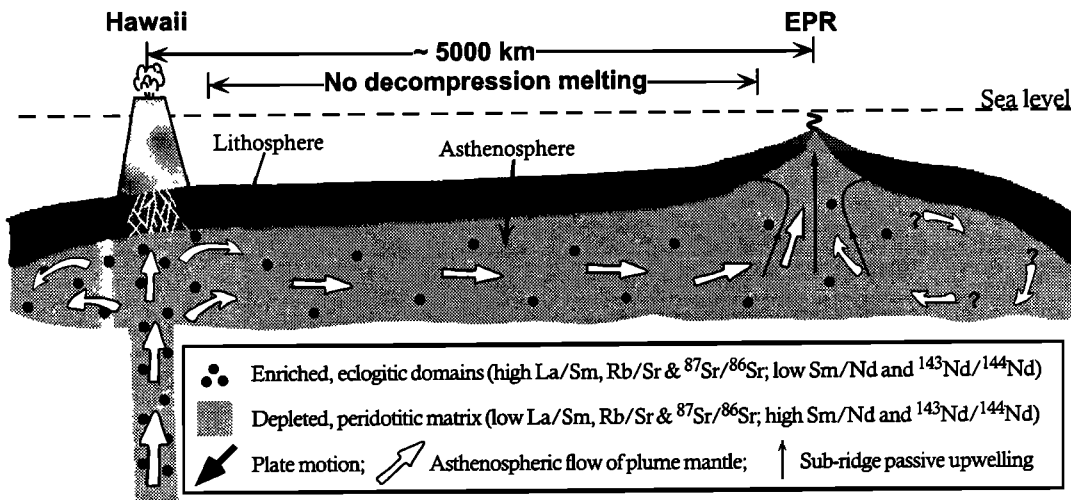


**Figure 13.** Cartoons showing different consequences of plume-ridge interactions as a function of distance between the plume and the ridge. If the plume is close to a ridge, for example, Iceland plume-Reykjanes Ridge (other examples including Azores, Galapagos, and Easter, etc. [e.g., Schilling, 1991]), the buoyant upwelling and melting of the hot plume produces shallow ridge topography and enriched OIB-like basalts. The ambient subridge mantle upwelling allows the plume material to flow laterally and to melt because of decompression, producing basalts whose extent of enrichment declines in the flow direction as the amount of the enriched component in the flowing plume mantle diminishes. The flow continues, but the enriched geochemical signals in the basalts do not. If the plume is far from a ridge, for example, Hawaiian plume-EPR, the low-viscosity Hawaii plume material may flow laterally toward the EPR in response to plate separation and lithosphere accretion at the EPR [Phipps Morgan et al., 1995]. As the lateral flow is largely horizontal, decompression melting does not take place during flow, which allows the Hawaiian plume materials (both enriched and depleted) to survive long-distance transport to the EPR mantle. The schematic lava compositional variation along the Reykjanes Ridge is based on the data given by Sun et al. [1975] and Taylor et al. [1997].

consequences of melting a heterogeneous mantle are the same, resulting in similar mixing relationships in geochemical diagrams (e.g., Figures 3, 4, 6, and 8). However, we can infer that the recycled eclogites are the dominant enriched lithologies in the MORB source, whereas metasomatic dikes/veins are important in generating extremely enriched alkaline lavas in off-ridge seamounts [e.g., *Cousens*, 1996; *Batiza and Vanko*, 1984; *Zindler et al.*, 1984] and on many ocean islands (e.g., alkali basalts, nephelinite, basanite, etc. in Hawaiian Islands). If rideward asthenospheric flow of plume materials is important in feeding ridges [*Phipps Morgan et al.*, 1995], then the lack of decompression in the course of transport allows the Hawaiian plume materials (both enriched eclogitic lithologies and depleted matrix) to be carried to the EPR mantle (see Figure 13). However, volumetrically small low-degree melts enriched in volatiles ( $H_2O$  and  $CO_2$ ) and incompatible elements may inevitably develop in the low-velocity zone and migrate upward and metasomatize the cooling and growing lithosphere as fine dikes and veins [e.g., *Green*, 1971; *Sun and McDonough*, 1989]. The metasomatized/veined lithospheric mantle will be readily tapped by off-ridge seamount volcanism. This low-velocity zone metasomatism may be a widespread phenomenon and may have taken place throughout much of Earth's history [e.g., *Green*, 1991; *Sun and McDonough*, 1989]. The important implication is that reinjection of this metasomatized lithosphere into the mantle at subduction zones would contribute significantly to the enriched component in the sources of oceanic basalts. This process will certainly complicate the small-scale and large-amplitude mantle heterogeneity, which needs to be considered in comprehensive models of intraoceanic crust/mantle differentiation.

**4.7.2. Nature and composition of the depleted MORB mantle beneath the EPR.** *Batiza and Vanko* [1984] and *Zindler et al.* [1984] show that lavas from near-ridge seamounts in the northern EPR region vary considerably in composition from highly enriched alkali basalts to extremely depleted tholeiites, reflecting with great fidelity the nature and scale of the source heterogeneity in the sub-EPR mantle. *Niu and Batiza* [1997a] show that the most depleted seamount lavas have  $Zr/Hf \leq 25$ ,  $Nb/Ta \leq 10$ ,  $Th/U \leq 1.5$ ,  $Nb/U \leq 20$ ,  $Rb/Cs \leq 20$ , and  $Ce/Pb \leq 15$ , far lower than those of the most depleted N-type MORB [*Hofmann*, 1988; *Sun and McDonough*, 1989]. As the elements in the numerator are more incompatible than elements in the denominator [see *Niu and Batiza*, 1997a, Figure 7], these ratios must be even lower in the depleted source. Thus we can conclude with confidence that these ratios are maximum estimates of the highly depleted peridotitic matrix of the two-component mantle. The implication is that even the highly depleted MORB lavas are not purely derived from the peridotitic matrix but contain a component of the enriched lithologies of the two-component mantle. As the enriched lithologies are physically distinct domains, well stirred, but not homogenized with the depleted peridotitic matrix, we can conclude that radiogenic isotope compositions of average MORB must not be the same as those of the depleted peridotitic matrix. This is conceptually important for models of chemical differentiation, and, in particular, for efforts in studying osmium isotopes aimed at unravelling crust-mantle recycling. Abyssal peridotites, if identified to be unrefertilized by late-stage melt, should preserve pristine isotopic signatures of the depleted peridotitic matrix. Alternatively, the extremely depleted seamount lavas or lavas that are found in some unusual tectonic settings like the Garrett transform are also expected to provide reliable isotopic information on the depleted peridotitic matrix. In

the Garrett transform, the highly incompatible-element depleted lavas [*Hékinian et al.*, 1995; *Niu and Hékinian*, 1997] also show extraordinarily depleted isotopic signatures (see Figure 10) [*Hamelin et al.*, 1984; *Mahoney et al.*, 1994; *Wendt et al.*, 1997] because these lavas result from intratransform extension induced decompression melting of the depleted peridotitic matrix that had lost the easily melted enriched domains beneath the EPR [*Wendt et al.*, 1997].

**4.7.3. Origin of the EPR-type major element systematics.** *Niu and Batiza* [1991, 1993a] showed that on ridge segment scales, MORB from the EPR define positive  $Na_8-Si_8/Fe_8$  and negative  $Ca_8/Al_8-Si_8/Fe_8$  trends, which are parallel to the so-called global trend of *Klein and Langmuir* [1987, 1989]. The global trend has been interpreted to reflect mantle temperature variation [e.g., *Klein and Langmuir*, 1987, 1989; *Niu and Batiza*, 1991, 1993a; *Langmuir et al.*, 1992]. However, as it is difficult to maintain large lateral thermal gradients in the mantle solidus depth on spatial scales as short as a few tens of kilometers for a prolonged period, it is unlikely that mantle temperature variation is the cause of the observed "global trend" defined by the segment-scale EPR lavas. From Figure 6, it is readily seen that a negative  $Na_{72}-Fe_{72}$  correlation and a positive  $Ca_{72}/Al_{72}-Fe_{72}$  correlation exist for the  $11^{\circ}20'N$  data, and all these parameters also correlate significantly with  $[La/Sm]_N$ ,  $[Sm/Yb]_N$ , and  $^{87}Sr/^{86}Sr$ . These correlations apply to the large seamount data set as well and thus clearly result from mantle source heterogeneities not mantle temperature variation, as suggested in this context by *Langmuir et al.* [1992].

**4.7.4. Origin of the "garnet signature" in MORB.** Partition coefficients of rare Earth elements (REEs) between garnet and basaltic melts increase systematically with atomic number and vary over 2 orders of magnitude, so that whereas light REEs are incompatible in garnet, heavy REEs are strongly compatible in garnet [*Irving and Frey*, 1978]. Consequently, high  $[Ce/Yb]_N$  and  $[Sm/Yb]_N$  ratios in basalts would suggest the presence of garnet as a residual phase in the source region that holds heavy REEs. Using regionally averaged REE data, *Shen and Forsyth* [1995] and many previous workers suggested that pressure-release melting beneath ocean ridges begins within the garnet-peridotite field ( $\geq 80$  km) as opposed to the spinel-peridotite field ( $\leq 80$  km). This interpretation is also supported by Hf isotope systematics [*Salter and Hart*, 1989] because  $Lu/Hf$  ratios in MORB are too low to explain the observed  $^{176}Hf/^{177}Hf$  ratios without invoking hidden Lu (held back by garnet in the source). However, although the garnet signature may be genetically related to garnet, it may not necessarily be a reliable indicator for decompression melting beginning within the garnet-peridotite field [*Hirschmann and Stolper*, 1996]. For example, it is readily seen from Figure 6 that the garnet signature (high  $[Sm/Yb]_N$ ) is associated with the enriched component and is a source signature. Neither the bulk of a two-component mantle nor the contained enriched eclogitic lithologies may have already possessed the garnet signature, but fractional or incremental melts produced by progressive partial melting of the eclogite-containing mantle will acquire the garnet signature. The "intensity" of the garnet signature in erupted basalts is thus expected to be proportional to the amount of these enriched eclogitic lithologies present in the MORB source (Figure 6) or inversely related to the extent of dilution; it would be diluted less in basalts produced by low ambient extents of melting (e.g., the Australian Antarctic Discordance and Cayman Rise) than in basalts produced by high ambient extents of melting (e.g., Kolbeinsey Ridge and Reykjanes

Ridge). A positive  $[\text{Sm}/\text{Yb}]_N\text{-Na}_{8(\text{or } 72)}$  correlation (Figure 6) is thus expected without having to invoke varying final depth of melting [Shen and Forsyth, 1995] or changing melting region shape [Salters, 1996].

## 5. Summary

The major results of this study are the following:

1. The significant correlations among Sr-Nd isotopes, incompatible trace elements, and major elements in the  $11^\circ 20' \text{N}$  EPR data confirm previous suggestions that the sub-EPR mantle contains two components: the enriched component occurs as physically distinct domains, widely but irregularly dispersed in the ambient depleted matrix.

2. The enriched component and the depleted matrix both possess high Nb (vs. Th) and Ta (vs. U), suggesting that they both are constituents of recycled oceanic lithosphere and have lost Th (vs. Nb) and U (vs. Ta) during subduction zone dehydration that preferentially transfers water-soluble Th and U to the mantle wedge above for arc volcanism and leaves the residual subducted lithosphere depleted in Th and U. Return of the residual lithosphere to the sources of oceanic basalts gives rise to the high Nb (vs. Th) and Ta (vs. U) in these basalts.

3. The recycled oceanic crustal lithologies (i.e., eclogites consisting of garnet and clinopyroxene) are the major source of the enriched component, whereas the recycled, previously melt-depleted peridotitic residues underlying the crust are the most depleted end-member. These two types of lithologies in the recycled oceanic lithosphere may be well stirred yet not homogenized during the course of mantle circulation, forming the "marble cake" structure of the two-component mantle.

4. As all MORB we have discussed, even the most depleted lavas are derived from this well-stirred two-component mantle; they thus always contain an element of the enriched component. Therefore radiogenic isotope compositions of average MORB are not expected to be the same as those of the depleted peridotitic matrix. This is conceptually important for models of chemical differentiation and, in particular, for efforts in studying Os isotopes aimed at revealing crust-mantle recycling.

5. The Pb-Sr isotopic relationship of the  $11^\circ 20' \text{N}$  lavas suggests that the enriched material may have actually flowed laterally from the Hawaiian hotspot, as suggested by mantle tomographic studies, although the nature of the flow process is uncertain and the direction of flow (opposite to plate motion) and the long distance between Hawaii and the EPR make such transport seemingly difficult. However, we believe that passive lateral flow of low-viscosity materials through the low-velocity zone to feed a ridge in response to plate separation and lithosphere accretion is physically more likely than passive vertical flow of high-viscosity materials from depth. The long distance of transport between Hawaii and the EPR can explain both the random distribution (vs. spatial gradient) of the E-type MORB and the absence of apparent thermal effects (e.g., regional topographic anomalies) at the EPR. Importantly, as the asthenospheric flow is largely horizontal, decompression melting thus does not take place during flow. Therefore Hawaiian plume materials (both enriched and depleted) can survive long-distance transport to the EPR mantle. This hypothesis should be testable by means of geophysical fluid dynamics and by examination of Pb and helium isotopes on samples from the broad northern EPR region.

6. The so-called garnet signature in MORB is interpreted to be a source characteristic and result from partial melting of the

eclogite-containing two-component mantle. The "intensity" of the garnet signature in basalts would be proportional to the amount of the enriched eclogitic lithologies present in the MORB source and would be diluted more in basalts produced by high ambient extents of melting (e.g., Kolbeinsey Ridge) than in basalts produced by low ambient extents of melting (e.g., the AAD and Cayman Rise) without having to invoke varying final depth of melting or changing melting region shape.

7. The positive correlation on  $\text{Na}_8\text{-Si}_8/\text{Fe}_8$  space and negative correlation on  $\text{Ca}_8/\text{Al}_8\text{-Si}_8/\text{Fe}_8$  space defined by the EPR lavas, which are parallel to the so-called global trend, are clearly caused by mantle source compositional variation not mantle temperature variation.

**Acknowledgments.** We thank the captain and crew of the R/V *Melville* during Phoenix 02 expedition and our fellow shipmates for helping obtain the samples. The sampling was supported by NSF and ONR, and laboratory work was supported by The University of Queensland NSRG and ARC grants. We thank Tony Ewart and Shen-su Sun for helpful discussions. Constructive reviews by Don Francis, Fred Frey, and an anonymous reviewer are acknowledged with gratitude. This is SOEST contribution 4679.

## References

- Aggrey, K. E. D., D. W. Muenow, and R. Batiza, Volatile abundances in basaltic glasses from seamounts flanking the East Pacific Rise at  $21^\circ\text{-}14^\circ\text{N}$ , *Geochim. Cosmochim. Acta*, **52**, 2115-2119, 1988.
- Albarède, F., High-resolution geochemical stratigraphy of Mauna Kea flows from the Hawaii Scientific Drilling Project core, *J. Geophys. Res.*, **101**, 11,841-11,853, 1996.
- Allègre, C. J., and D. L. Turcotte, Implications of a two-component marble-cake mantle, *Nature*, **323**, 123-127, 1986.
- Allègre, C. J., B. Hamelin, and B. Dupré, Statistical analyses of isotopic ratios in MORB: The mantle blob cluster model and the convective regime of the mantle, *Earth Planet. Sci. Lett.*, **71**, 71-84, 1984.
- Allègre, C. J., B. Dupré, and E. Lewin, Thorium/uranium ratio of the Earth, *Chem. Geol.*, **56**, 219-227, 1986.
- Bach, W., E. Hegner, E. Erzinger, and M. Satir, Chemical and isotopic variations along the superfast spreading East Pacific Rise from  $6^\circ$  to  $30^\circ\text{S}$ , *Contrib. Mineral. Petrol.*, **116**, 365-380, 1994.
- Baker, M. B., and E. M. Stolper, Determining the composition of high-pressure mantle melts using diamond aggregates, *Geochim. Cosmochim. Acta*, **58**, 2811-2827, 1994.
- Baker, M. B., M. M. Hirschmann, M. S. Ghiorso, and E. M. Stolper, Compositions of near-solidus peridotite melts from experiments and thermodynamic calculations, *Nature*, **375**, 308-311, 1995.
- Batiza, R., and Y. Niu, Petrology and magma chamber processes at the East Pacific Rise  $\sim 9^\circ 30' \text{N}$ , *J. Geophys. Res.*, **97**, 6779-6797, 1992.
- Batiza, R., and D. A. Vanko, Petrology of young Pacific seamounts, *J. Geophys. Res.*, **89**, 11,235-11,260, 1984.
- Batiza, R., et al., Temporal variation of East Pacific Rise lavas to  $0.5 \text{ Ma}$  at  $\sim 9^\circ 30' \text{N}$ ,  $\sim 10^\circ \text{N}$ , and  $\sim 11^\circ 20' \text{N}$  (abstract), *Eos Trans. AGU*, **73(43)**, Fall Meet. Suppl., 525, 1992.
- Batiza, R., Y. Niu, J. L. Karsten, W. Boger, E. Potts, L. Norby, and R. Butler, Steady and non-steady state magma chambers below the East Pacific Rise, *Geophys. Res. Lett.*, **23**, 221-224, 1996.
- Bideau, D., and R. Hékinian, A dynamic model for generating small-scale heterogeneities in ocean floor basalts, *J. Geophys. Res.*, **100**, 10,141-10,162, 1995.
- Carmichael, I. S. E., F. J. Turner and J. Verhoogen, *Igneous Petrology*, McGraw-Hill, New York, 1974.
- Castillo, P. R., W. White, K. Harpp, R. Batiza, and Y. Niu, Petrology and Sr, Nd, and Pb isotope geochemistry of MORB from the  $14^\circ$  to  $15^\circ \text{N}$  segment of the EPR (abstract), *Eos Trans. AGU*, **72(44)**, Fall Meet. Suppl., 525, 1991.
- Christensen, U., Effects of phase transformations on mantle convection, *Annu. Rev. Earth Planet. Sci.*, **23**, 65-87, 1995.
- Cohen, R. S., and R. K. O'Nions, The lead, neodymium and strontium isotopic structure of ocean ridge basalts, *J. Petrol.*, **23**, 299-324, 1982.
- Cousens, B. L., Depleted and enriched upper mantle sources for basaltic rocks from diverse tectonic environments in the northeast Pacific ocean: The generation of oceanic alkaline vs. tholeiitic basalts, in *Earth Processes: Reading the Isotopic Code*, *Geophys. Monogr. Ser.*,

- vol. 95, edited by A. Basu and S. Hart, pp. 207-231, AGU, Washington, D.C., 1996.
- Davies, G. F., Ocean bathymetry and mantle convection, I, Large-scale flow and hotspots, *J. Geophys. Res.*, **93**, 10,467-10,480, 1988.
- Dosso, L., H. Bougault, and J.-L. Joron, Geochemical morphology of the North Mid-Atlantic Ridges, 10°-24°N: Trace element-isotope complementary, *Earth Planet. Sci. Lett.*, **120**, 443-462, 1993.
- Duncan, R. A., and L. G. Hogan, Radiometric dating of young MORB using <sup>40</sup>Ar-<sup>39</sup>Ar incremental heating method, *Geophys. Res. Lett.*, **21**, 1927-1930, 1994.
- Dupré, B., and C. J. Allègre, Pb-Sr isotope correlation in Indian Ocean basalts and mixing phenomena, *Nature*, **303**, 142-146, 1983.
- Ewart, A., K. D. Collerson, M. Regelous, J. I. Wendt, and Y. Niu, Geochemical evolution within the Tonga-Kermadec-Lau Arc-Backarc system: The role of varying mantle wedge composition in space and time, *J. Petrol.*, **39**, 331-368, 1998.
- Falloon, T. J., D. H. Green, C. J. Hatton, and K. L. Harris, Anhydrous partial melting of a fertile and depleted peridotite from 2 to 30 Kb and application to basalt petrogenesis, *J. Petrol.*, **29**, 1257-1282, 1988.
- Fitton, J. G., and D. James, Basic volcanism associated with intraplate linear features, *Philos. Trans. R. Soc. London, Ser. A*, **317**, 253-266, 1986.
- Frey, F. A., M. O. Garcia, and M. F. Roden, Geochemical characteristics of Koolau Volcano: Implications of intershield geochemical differences among Hawaiian volcanoes, *Geochim. Cosmochim. Acta*, **58**, 1441-1462, 1994.
- Gast, P. W., Trace element fractionation and the origin of tholeiitic and alkaline magma types, *Geochim. Cosmochim. Acta*, **32**, 1055-1086, 1968.
- Graham, D. W., A. Zindler, M. D. Kurz, W. J. Jenkins, R. Batiza, and H. Staudigel, He, Pb, Sr, and Nd isotope constraints on magma genesis and mantle heterogeneity beneath young Pacific seamounts, *Contrib. Mineral. Petrol.*, **99**, 446-463, 1988.
- Green, D. H., Composition of basaltic magmas as indicators of conditions of origin: Application to oceanic volcanism, *Philos. Trans. R. Soc. London, Ser. A*, **268**, 707-725, 1971.
- Green, D. H., The Earth's lithosphere and asthenosphere - Concepts and constraints derived from petrology and high pressure experiments, *Spec. Publ. Geol. Soc. Aust.*, **17**, 1-22, 1991.
- Hamelin, B., B. Dupré, and C. J. Allègre, Lead-strontium isotopic variations along the East Pacific Rise and Mid-Atlantic Ridge: A comparative study, *Earth Planet. Sci. Lett.*, **67**, 340-350, 1984.
- Hanan, B. B., and D. W. Graham, Lead and helium isotope evidence from oceanic basalts for a common deep source of mantle plumes, *Science*, **272**, 991-995, 1996.
- Hanan, B. B., R. H. Kinsley, and J.-G. Schilling, Pb isotope evidence in the South Atlantic for migrating ridge-hotspot interactions, *Nature*, **322**, 137-144, 1986.
- Hanson, G. N., Geochemical evolution of the suboceanic mantle, *J. Geol. Soc. London*, **134**, 235-253, 1977.
- Hart, S., and A. Zindler, Constraints on the nature and development of chemical heterogeneities in the mantle, in *Mantle Convection*, edited by W. R. Peltier, pp. 262-387, Gordon and Breach, Newark, N. J., 1989.
- Hart, S. R., E. H. Hauri, L. A. Oschmann, and J. A. Whitehead, Mantle plumes and entrainment: Isotopic evidence, *Science*, **256**, 517-520, 1992.
- Hauri, E. H., Major element variability in the Hawaiian mantle plume, *Nature*, **382**, 415-419, 1996.
- Hékinian, R., G. Thompson, and D. Bideau, Axial and off-axial heterogeneity of basaltic rocks from the East Pacific Rise at 12°35'N-12°51'N and 11°26'N-11°30'N, *J. Geophys. Res.*, **94**, 17,437-17,463, 1989.
- Hékinian, R., D. Bideau, R. Herbért, and Y. Niu, Magmatism in the Garrett transform fault (East Pacific Rise near 13°27'S), *J. Geophys. Res.*, **100**, 10,163-10,185, 1995.
- Hirschmann, M. M., and E. M. Stolper, A possible role for garnet pyroxenite in the origin of the "garnet signature" in MORB, *Contrib. Mineral. Petrol.*, **124**, 185-208, 1996.
- Hofmann, A. W., Chemical differentiation of the Earth: The relationship between mantle, continental crust, and oceanic crust, *Earth Planet. Sci. Lett.*, **90**, 297-314, 1988.
- Hofmann, A. W., Mantle geochemistry: The message from oceanic volcanism, *Nature*, **385**, 219-229, 1997.
- Hofmann, A. W., and K. P. Jochum, Source characteristics derived from very incompatible trace elements in Mauna Loa and Mauna Kea basalts, Hawaii Scientific Drilling Project, *J. Geophys. Res.*, **101**, 11,831-11,839, 1996.
- Hofmann, A. W., and W. M. White, Mantle plumes from ancient oceanic crust, *Earth Planet. Sci. Lett.*, **57**, 421-436, 1982.
- Hofmann, A. W., K. P. Jochum, M. Seufert, and W. M. White, Nb and Pb in oceanic basalts: New constraints on mantle evolution, *Earth Planet. Sci. Lett.*, **79**, 33-45, 1986.
- Irving, A. J., and F. A. Frey, Distribution of trace elements between garnet megacrysts and host volcanic liquids of kimberlitic to rhyolitic composition, *Geochim. Cosmochim. Acta*, **42**, 771-787, 1978.
- Ito, E., W. M. White, and C. Göpel, The O, Sr, and Pb isotope geochemistry of MORB, *Chem. Geol.*, **62**, 157-176, 1987.
- Ito, G., and J. Lin, Oceanic spreading center-hotspot interactions: Constraints from along-isochron bathymetric and gravity anomalies, *Geology*, **23**, 657-660, 1995.
- Ito, G., J. Lin, and C. W. Gable, Dynamics of mantle flow and melting at a ridge-centered hotspot: Iceland and the Mid-Atlantic Ridge, *Earth Planet. Sci. Lett.*, **144**, 53-74, 1996.
- Janney, P. E., and P. R. Castillo, Geochemistry of Mesozoic Pacific mid-ocean ridge basalt: Constraints on melt generation and the evolution of the Pacific upper mantle, *J. Geophys. Res.*, **102**, 5207-5229, 1997.
- Jaques, A. L., and D. H. Green, Anhydrous melting of peridotite at 0-15 kb pressure and the genesis of tholeiitic basalts, *Contrib. Mineral. Petrol.*, **73**, 287-310, 1980.
- Kincaid, C., G. Ito, and C. Gable, Laboratory investigations of the interaction of off-axis mantle plumes and spreading centres, *Nature*, **376**, 758-761, 1995.
- Klein, E. M., and J. L. Karsten, Ocean-ridge basalts with convergent-margin geochemical affinities from the Chile Ridge, *Nature*, **374**, 52-57, 1995.
- Klein, E. M., and C. H. Langmuir, Global correlations of ocean ridge basalt chemistry with axial depth and crustal thickness, *J. Geophys. Res.*, **92**, 8089-8115, 1987.
- Klein, E. M., and C. H. Langmuir, Local versus global variation in ocean ridge basaltic composition: A reply, *J. Geophys. Res.*, **94**, 4241-4252, 1989.
- Kurz, M. D., W. J. Jenkins, S. R. Hart, and D. Clague, Helium isotopic variations in volcanic rocks from Loihi Seamount and the Island of Hawaii, *Earth Planet. Sci. Lett.*, **66**, 388-406, 1983.
- Kushiro, I., Partial melting of a fertile mantle peridotite at high pressures: An experimental study using aggregates of diamond, in *Earth Processes: Reading the Isotopic Code*, *Geophys. Monogr. Ser.*, vol. 95, edited by A. Basu and S. Hart, pp. 109-122, AGU, Washington, D.C., 1996.
- Kushiro, I., Y. Syono, and S. Akimoto, Melting of a peridotite nodule at high pressures and high water pressures, *J. Geophys. Res.*, **73**, 6023-6029, 1968.
- Langmuir, C. H., R. D. Vocke, G. N. Hanson, and S. R. Hart, A general mixing equation with application to Icelandic basalts, *Earth Planet. Sci. Lett.*, **37**, 380-392, 1978.
- Langmuir, C. H., J. F. Bender, and R. Batiza, Petrological and tectonic segmentation of the East Pacific Rise, 5°30'-14°30'N, *Nature*, **332**, 422-429, 1986.
- Langmuir, C. H., E. M. Klein, and T. Plank, Petrological systematics of mid-ocean ridge basalts: Constraints on melt generation beneath ocean ridges, in *Mantle Flow and Melt Generation at Mid-Ocean Ridges*, *Geophys. Monogr. Ser.*, vol. 71, edited by J. P. Morgan, D. K. Blackman, and J. M. Sinton, pp. 183-280, AGU, Washington, D.C., 1992.
- Le Roex, A. P., H. J. B. Dick, A. L. Erlank, A. M. Reid, F. A. Frey, and S. R. Hart, Geochemistry, mineralogy and petrogenesis of lavas erupted along the Southwest Indian Ridge between the Bouvet Triple Junction and 11 degrees east, *J. Petrol.*, **24**, 267-318, 1983.
- Le Roex, A. P., H. J. B. Dick, A. L. Erlank, A. M. Reid, F. A. Frey, and S. R. Hart, Petrology and geochemistry of basalts from the American-Antarctic Ridge, southern ocean: Implications for the westward influence of the Bouvet mantle plume, *Contrib. Mineral. Petrol.*, **90**, 367-380, 1985.
- Macdonald, K. C., P. J. Fox, L. J. Perram, M. F. Eisen, R. M. Haymon, S. P. Miller, S. M. Carbotte, M.-H. Cormier, and A. N. Shor, A new view of the mid-ocean ridge from the behavior of ridge-axis discontinuities, *Nature*, **335**, 217-225, 1988.
- Macdougall, J. D., and G. W. Lugmair, Sr and Nd isotopes in basalts from the East Pacific Rise: Significance for mantle heterogeneity, *Earth Planet. Sci. Lett.*, **77**, 273-289, 1986.
- Mahoney, J. J., J. H. Natland, W. M. White, R. Poreda, S. H. Bloomer, R. L. Fisher, and A. N. Baxter, Isotopic and geochemical provinces of the

- western Indian Ocean spreading centers, *J. Geophys. Res.*, *94*, 4033-4052, 1989.
- Mahoney, J. J., J. M. Sinton, D. M. Kurz, J. D. Macdougall, K. J. Spencer, and G. W. Lugmair, Isotope and trace element characteristics of a super-fast spreading ridge: East Pacific Rise, 13 - 23°S, *Earth Planet. Sci. Lett.*, *121*, 173-193, 1994.
- McDonough, W. F., Partial melting of subducted oceanic crust and isolation of its residual eclogitic lithology, *Philos. Trans. R. Soc. London, Ser. A*, *335*, 407-418, 1991.
- Melson, W. G., T. L. Vallier, T. L. Wright, G. Byerly, and J. Nelen, Chemical diversity of abyssal volcanic glass erupted along Pacific, Atlantic and Indian Ocean sea-floor spreading centers, in *The Geophysics of the Pacific Ocean and its Margin: A Volume in Honor of George P. Woollard, Geophys. Monogr. Ser.*, vol. 19, edited by G. H. Sutton, M. H. Manghni, and R. Moberly, pp. 351-368, AGU, Washington, D. C., 1976.
- Michael, P. J., Regionally distinctive sources of depleted MORB: Evidence from trace elements and H<sub>2</sub>O, *Earth Planet. Sci. Lett.*, *131*, 301-320, 1995.
- Michael, P. J., et al., Mantle control of a dynamically evolving spreading center, *Earth Planet. Sci. Lett.*, *121*, 451-468, 1994.
- Morgan, J. W., and J. Phipps Morgan, Two-stage melting of a multi-component mantle: A way to generate both OIB and MORB from 'whole mantle' convection (abstract), *Terra Nova Abstr.*, *9*, 57, 1997.
- Mysen, B. O., and A. L. Boettcher, Melting of a hydrous mantle: II. Geochemistry of crystals and liquids formed by anatexis of mantle peridotite at high pressures and high temperatures as a function of controlled activities of water, hydrogen, and carbon dioxide, *J. Petrol.*, *16*, 549-593, 1975.
- Natland, J. H., Partial melting of a lithologically heterogeneous mantle: Inferences from crystallisation histories of magnesian abyssal tholeiites from the Siqueiros Fracture Zone, in *Magmatism in the Ocean Basins*, edited by A. D. Saunders, and M. J. Norry, *Geol. Soc. Spec. Pub.*, *42*, pp. 41-70, 1989.
- Niu, Y., and R. Batiza, An empirical method for calculating melt compositions produced beneath mid-ocean ridges: Application for axis and off-axis (seamounts) melting, *J. Geophys. Res.*, *96*, 21,753-21,777, 1991.
- Niu, Y., and R. Batiza, Chemical variation trends at fast and slow spreading ridges, *J. Geophys. Res.*, *98*, 7887-7902, 1993a.
- Niu, Y., and R. Batiza, Magmatic variability of the East Pacific Rise at 9°30'N, 10°30'N, and 11°20'N over the last 600 Ka (abstract), *Eos Trans. AGU*, *74*(16), Spring Meet. Suppl., 297, 1993b.
- Niu, Y., and R. Batiza, Trace element evidence from seamounts for recycled oceanic crust in the eastern equatorial Pacific mantle, *Earth Planet. Sci. Lett.*, *148*, 471-484, 1997a.
- Niu, Y., and R. Batiza, Extreme mantle source heterogeneities beneath the northern East Pacific Rise - Trace element evidence from near-ridge seamounts, in *Igneous Petrology*, edited by Z. Li, *Proc. 30th Int. Geol. Congr.*, *15*, 109-120, 1997b.
- Niu, Y., and R. Hékinian, Basaltic liquids and harzburgitic residues in the Garrett Transform: A case study at fast-spreading ridges, *Earth Planet. Sci. Lett.*, *146*, 243-258, 1997.
- Niu, Y., K. D. Collerson, and R. Batiza, Temporal variability of mantle source heterogeneity beneath the East Pacific Rise at 11°20'N over the last 600 Ka, *Eos Trans. AGU*, *75*(44), Fall Meet. Suppl., 742, 1994.
- Niu, Y., D. G. Wagoner, J. M. Sinton and J. J. Mahoney, Mantle source heterogeneity and melting processes beneath seafloor spreading centers: The East Pacific Rise, 18° - 19°S, *J. Geophys. Res.*, *101*, 27,711-27,733, 1996.
- O'Nions, R. K., P. J. Hamilton, and N. M. Evensen, Variations in <sup>143</sup>Nd/<sup>144</sup>Nd and <sup>87</sup>Sr/<sup>86</sup>Sr ratios in oceanic basalts, *Earth Planet. Sci. Lett.*, *34*, 13-22, 1977.
- Pan, Y., and R. Batiza, Major element chemistry of volcanic glasses from the Easter Seamount Chain: Constraints on melting conditions in the plume channel, *J. Geophys. Res.*, *103*, 5287-5304, 1998.
- Pearce, J. A., and D. W. Peate, Tectonic implications of the composition of volcanic arc magmas, *Annu. Rev. Earth Planet. Sci.*, *23*, 251-285, 1995.
- Perfit, M. R., D. J. Fornari, M. C. Smith, J. F. Bender, C. H. Langmuir, and R. M. Haymon, Small-scale spatial and temporal variations in mid-ocean ridge crest magmatic processes, *Geology*, *22*, 375-379, 1994.
- Phipps Morgan, J., and J. W. Morgan, Rare gas and isotope evolution of the mantle (abstract), *Terra Nova Abstr.*, *9*, 47, 1997.
- Phipps Morgan, J., W. J. Morgan, Y.-S. Zhang, and W. H. F. Smith, Observational hints for a plume-fed, suboceanic asthenosphere and its role in mantle convection, *J. Geophys. Res.*, *100*, 12,753 - 12,767, 1995.
- Prinzhofer, A., E. Lewin, and C. J. Allègre, Stochastic melting of the marble cake mantle: Evidence from local study of the East Pacific Rise at 12°50'N, *Earth Planet. Sci. Lett.*, *92*, 189-206, 1989.
- Regelous, M., K. D. Collerson, A. Ewart, and J. I. Wendt, Trace element transport rates in subduction zones - Evidence from Th, Sr and Pb isotopes, *Earth Planet. Sci. Lett.*, *150*, 291-302, 1997a.
- Regelous, M., Y. Niu, J. I. Wendt, R. Batiza, A. Grieg, and K. D. Collerson, Geochemistry of magmatism on the EPR at 10°30'N, 800 ka to present Insights into magma chamber processes (abstract), *Eos Trans. AGU*, *78*(46), Fall Meet. Suppl., F657, 1997b.
- Reynolds, J. R., C. H. Langmuir, J. F. Bender, K. A. Kastens, and W. B. F. Ryan, Spatial and temporal variability in the geochemistry of basalts from the East Pacific Rise, *Nature*, *359*, 493-499, 1992.
- Ribe, N. M., The dynamics of plume-ridge interaction, 2, Off-ridge plumes, *J. Geophys. Res.*, *101*, 16,195-16,204, 1996.
- Roden, M. F., T. Trull, S. R. Hart, and F. A. Frey, New He, Nd, Pb, and Sr isotopic constraints on the constitution of the Hawaiian plume: Results from Koolau Volcano, Oahu, Hawaii, USA, *Geochim. Cosmochim. Acta*, *58*, 1431-1440, 1994.
- Rudnick, R. L., and D. M. Fountain, Nature and composition of the continental crust: A lower crustal perspective, *Rev. Geophys.*, *33*, 267-309, 1995.
- Salters, V. J. M. The generation of mid-ocean ridge basalts from the HF and Nd isotope perspective, *Earth Planet. Sci. Lett.*, *141*, 109-123, 1996.
- Salters, V. J. M. and S. R. Hart, The hafnium paradox and the role of garnet in the source of mid-ocean ridge basalts, *Nature*, *342*, 420-422, 1989.
- Saunders, A. D., M. J. Norry, and J. Tarney, Origin of MORB and chemically-depleted mantle reservoirs: Trace element constraints, *J. Petrol.*, *29*, 415-445, 1988.
- Scheirer, D. S., and K. C. Macdonald, Variation in cross-sectional area of the axial ridge along the East Pacific Rise: Evidence for the magmatic budget of a fast spreading center, *J. Geophys. Res.*, *98*, 7871-7885, 1993.
- Schilling, J.-G., Fluxes and excess temperatures of mantle plumes inferred from their interaction with migrating mid-ocean ridges, *Nature* *352*, 397-403, 1991.
- Schilling, J.-G., M. Zajac, R. Evans, T. Johnston, W. White, J. D. Devine, and R. Kingsley, Petrological and geochemical variations along the Mid-Atlantic Ridge from 29°N to 73°N, *Am. J. Sci.*, *283*, 510-586, 1983.
- Shen, Y., and D. W. Forsyth, Geochemical constraints on initial and final depth of melting beneath mid-ocean ridges, *J. Geophys. Res.*, *100*, 2211-2237, 1995.
- Sinton, J. M., S. M. Smaglik, and J. J. Mahoney, Magmatic processes at superfast spreading mid-ocean ridges: Glass compositional variations along the East Pacific Rise 13°-23°S, *J. Geophys. Res.*, *96*, 6133-6155, 1991.
- Sleep, N. H., Tapping of magmas from ubiquitous mantle heterogeneities: An alternative to mantle plumes?, *J. Geophys. Res.*, *89*, 10,029 - 10,041, 1984.
- Sleep, N. H., Hotspots and mantle plumes: Some phenomenology, *J. Geophys. Res.*, *95*, 6715-6736, 1990.
- Sleep, N. H., Lateral flow of hot plume material ponded at sublithospheric depths, *J. Geophys. Res.*, *101*, 28,065-28,083, 1996.
- Staudigel, H., A. Zindler, S. R. Hart, T. Leslie, C.-Y. Chen, and D. Clague, The isotope systematics of a juvenile intraplate volcano: Pb, Nd, and Sr isotope ratios of basalts from Loihi seamount, Hawaii, *Earth Planet. Sci. Lett.*, *69*, 13-29, 1984.
- Stille, P., D. M. Unruh, and M. Tatsumoto, Pb, Sr, Nd, and Hf isotopic constraints on the origin of Hawaiian basalts and evidence for a unique mantle source, *Geochim. Cosmochim. Acta*, *50*, 2303-2319, 1986.
- Storey, M., A. D. Saunders, J. Tarney, I. L. Gibson, M. J. Norry, M. F. Thirlwall, P. Leat, R. N. Thompson, and M. A. Menzies, Contamination of the Indian Ocean asthenosphere by the Kerguelen-Heard mantle plume, *Nature*, *338*, 574-576, 1989.
- Sun, S.-S., and G. N. Hanson, Origin of Ross Island basanitoids and limitations upon the heterogeneity of mantle sources for alkali basalts and nephelinites, *Contrib. Mineral. Petrol.*, *52*, 77-106, 1975.
- Sun, S.-S., and W. F. McDonough, Chemical and isotopic systematics of ocean basalt: Implications for mantle composition and processes, in *Magmatism of the Ocean Basins*, edited by A. D. Saunders, and M. J. Norry, *Geol. Soc. Spec. Publ.*, *42*, 323-345, 1989.
- Sun, S.-S., M. Tatsumoto, and J.-G. Schilling, Mantle plume mixing along

- the Reykjanes ridge axis: Lead isotope evidence, *Science*, *190*, 143-147, 1975.
- Taylor, R. N., M. F. Thirwall, B. J. Morton, D. R. Hilton, and M. A. M. Gee, Isotopic constraints on the influence of the Icelandic plume, *Earth Planet. Sci. Lett.*, *148*, E1-E8, 1997.
- Taylor, S. R., and S. M. McLennan, *The Continental Crust: Its Composition and Evolution*, Blackwell, Cambridge, Mass., 1985.
- Thompson, G., W. B. Bryan, and S. E. Humphris, Axial volcanism on the East Pacific Rise, 10° - 12°N, in *Magmatism of the Ocean Basins*, edited by A. D. Saunders, and M. J. Norry, *Geol. Soc. Spec. Publ.*, *42*, 181-200, 1989.
- Thompson, R. N., G. L. Hendry, and S. J. Parry, An assessment of the relative roles of crust and mantle in magma genesis: An elemental approach, *Philos. Trans. R. Soc. London, Ser. A*, *310*, 549-590, 1984.
- van der Hilst, R. D., Evidence for deep mantle circulation from global tomography, *Nature*, *386*, 578-584, 1997.
- Vidal, P., and N. Clauer, Pb and Sr isotopic systematics of some of basalts and sulfides from the East Pacific Rise at 21°N (project RITA), *Earth Planet. Sci. Lett.*, *55*, 237-246, 1981.
- Weaver, B. L., The origin of ocean island basalt end-member compositions: Trace element and isotopic constraints, *Earth Planet. Sci. Lett.*, *104*, 381-397, 1991.
- Wendt, J. I., M. Regelous, R. Hékinian, Y. Niu, and K. D. Collerson, The nature of mantle source heterogeneities and melt extraction processes beneath the East Pacific Rise (EPR): Evidence from ultra-depleted lavas in the Garrett transform (abstract), *Eos Trans. AGU*, *78*(46), Fall Meet. Suppl., F675, 1997.
- West, H. B., M. O. Garcia, D. C. Gerlach, and J. Romano, Geochemistry of tholeiites from Lanai, Hawaii, *Contrib. Mineral. Petrol.*, *112*, 520-542, 1992.
- White, W. M., and R. A. Duncan, Geochemistry and geochronology of the Society Islands: New evidence for deep mantle recycling, in *Earth Processes: Reading the Isotopic Code*, *Geophys. Monogr. Ser.*, vol. 95, edited by A. Basu and S. Hart, pp. 183-206, AGU, Washington, D.C., 1996.
- White, W. M., and A. W. Hofmann, Sr and Nd isotope geochemistry of oceanic basalts and mantle evolution, *Nature*, *296*, 821-825, 1982.
- White, W. M., A. W. Hofmann, and H. Puchelt, Isotope geochemistry of Pacific mid-ocean ridge basalt, *J. Geophys. Res.*, *92*, 4881-4893, 1987.
- Wood, D. A., A variably veined suboceanic upper mantle - Genetic significance for mid-ocean ridge basalts from geochemical evidence, *Geology*, *7*, 499-503, 1979.
- Zhang, Y.-S., and T. Taniimoto, High-resolution global upper mantle structure and plate tectonics, *J. Geophys. Res.*, *98*, 9793-9823, 1993.
- Zindler, A., and S. R. Hart, Chemical geodynamics, *Annu. Rev. Earth Planet. Sci.*, *14*, 493-571, 1986.
- Zindler, A., H. Staudigel, and R. Batiza, Isotope and trace element geochemistry of young Pacific seamounts: Implications for the scale of upper mantle heterogeneity, *Earth Planet. Sci. Lett.*, *70*, 175-195, 1984.

---

R. Batiza, Department of Geology and Geophysics, School of Ocean and Earth Science and Technology, University of Hawaii, 2525 Correa Road, Honolulu, HI 96822-2399. (rbatiza@akule.soest.hawaii.edu)

K.D. Collerson, Y. Niu, M. Regelous, and J.I. Wendt, Department of Earth Sciences, The University of Queensland, Brisbane, Qld 4072, Australia. (niu@earthsciences.uq.edu.au)

(Received August 28, 1998; revised September 16, 1998; accepted September 25, 1998.)